Congress on Numerical Methods in Engineering 2022
12-14 Septiembre 2022, Las Palmas de Gran Canaria, España

Vertical dynamic interaction between suction caissons in tetrapod arrangements for offshore wind turbines

Jacob D.R. Bordón*, Fidel García, Luis A. Padrón, Juan J. Aznárez and Orlando Maeso

* Instituto Universitario de Sistemas Inteligentes y Aplicaciones Numéricas en Ingeniería
Universidad de Las Palmas de Gran Canaria
Campus Universitario de Tafira, Las Palmas de Gran Canaria 35017, Spain
e-mails:{jacobdavid.rodriguezbordon, fidel.garcia, juanjose.aznarez, orlando.maeso}@ulpgc.es

ABSTRACT

Offshore wind energy is playing an important role in the future mix of renewable sources for electrical power production. Although floating technology is taking off in a powerful way, more mature fixed wind turbines are still strongly growing in number and capabilities [1]. For challenging soft soils, suction caissons are often considered for geotechnical and ease of installation/removal reasons. In this contribution, the vertical dynamic interaction of a tetrapod arrangement of suctions caissons is studied through an specially tailored boundary element - shell finite element coupled model. The model is an evolution of a previous one [2], where the boundary element hypersingular formulation required to deal with the shell coupling is no longer needed, and an already available multilayered viscoelastic half-space Green's function [3] can be hence used. The discretization is thus reduced to only the suction caisson skirt and lid. The dynamic interaction is observed from the point of view of stiffnesses. The influence of the foundation spacing and soil properties on the resulting impedance matrix is studied. As expected, the most relevant factor on the dynamic interaction is the spacing. Impedance curves contain local minima and maxima at frequencies corresponding to wavelength fractions of the spacing.

ACKNOWLEDGMENTS

This work has been supported by the research project PID2020-120102RB-I00, funded by the Agencial Estatal de Investigación of Spain, MCIN/AEI/10.13039/501100011033.

REFERENCES

[1] EWEA (The European Wind Energy Association). Offshore Wind in Europe: Key trends and statistics 2020. Wind Europe, 2021.

[2] J.D.R Bordón, J.J. Aznárez, O. Maeso. Dynamic model of open shell structures buried in poroelastic soils. Computational Mechanics 60, 269–288, 2017.

[3] R.Y.S. Pak, B.B. Guzina. Three-dimensional Green's functions for a multilayered half-space in displacement potentials. Journal of Engineering Mechanics 128, 449–461, 2002.

Vertical dynamic interaction between suction caissons in tetrapod arrangements for offshore wind turbines

Jacob D.R. Bordón Fidel García Luis A. Padrón
Juan J. Aznárez Orlando Maeso

ULPGC
Universidad de Las Palmas de Gran Canaria
Instituto Universitario de Sistemas Inteligentes y Aplicaciones Numéricas en Ingenierías
SIANI

Congress on Numerical Methods in Engineering
CMN 2022
Las Palmas de Gran Canaria, Spain, 13 September, 2022

Outline

Outline

Offshore Wind Turbines (OWT)

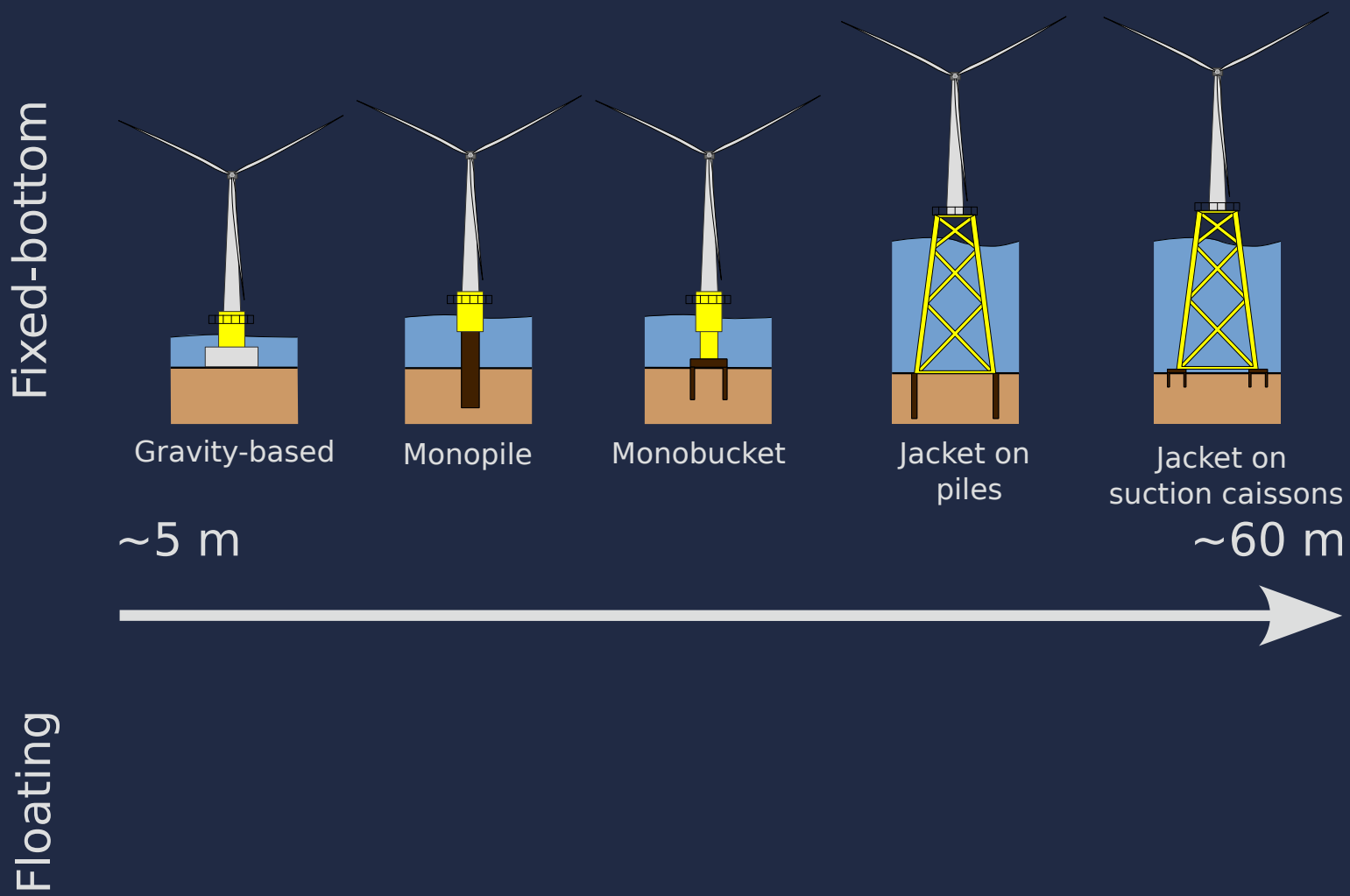

Offshore Wind Turbines (OWT)

Fixed-bottom

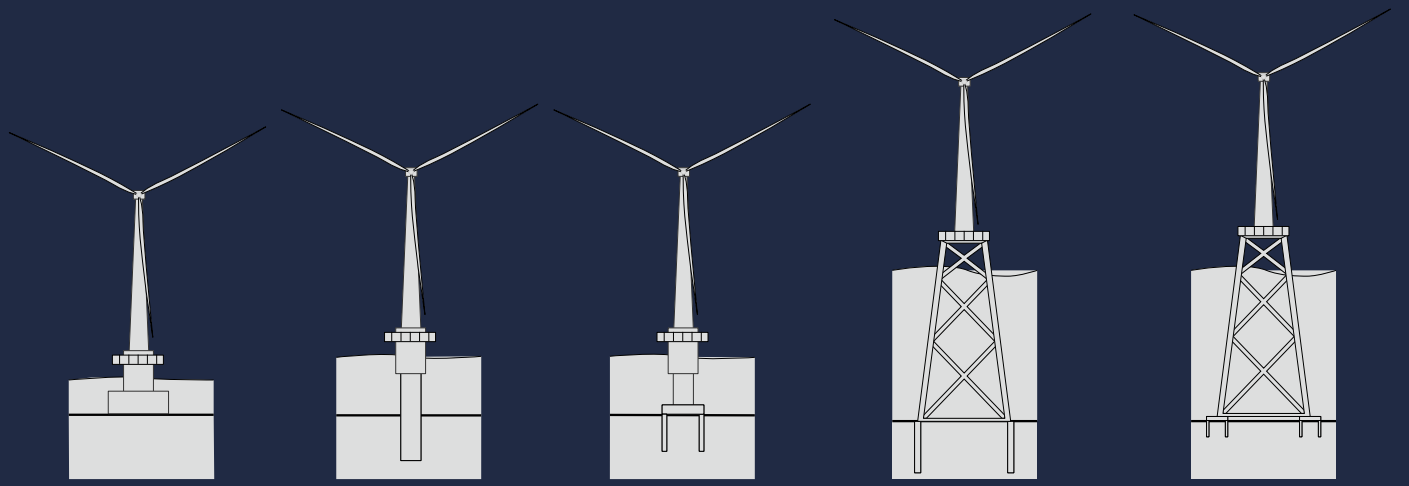

Gravity-based | Monopile | Monobucket | Jacket on piles | Jacket on suction caissons

Floating

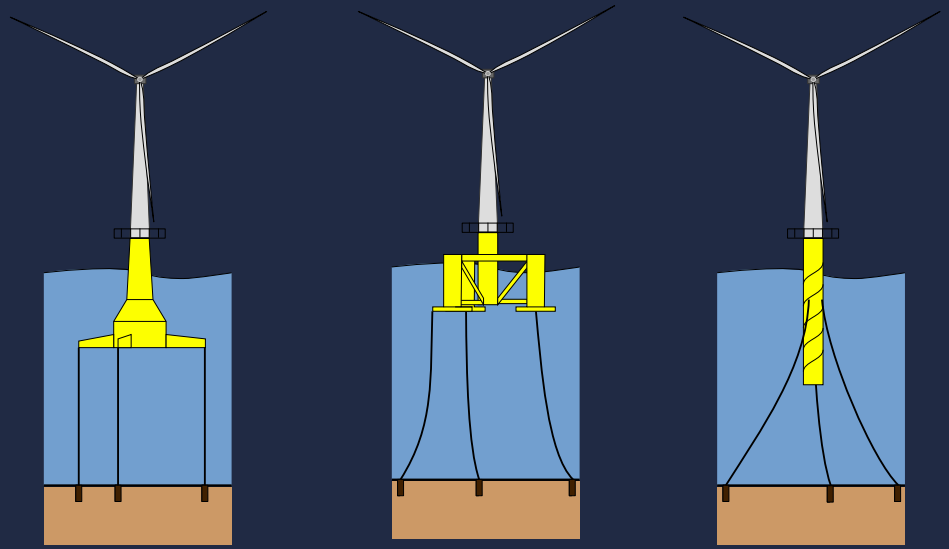

Tension-Leg Platform (TLP) | Semi-submersible | Spar

~60 m
to
~300 m

Offshore Wind Turbines (OWT)

Fixed-bottom

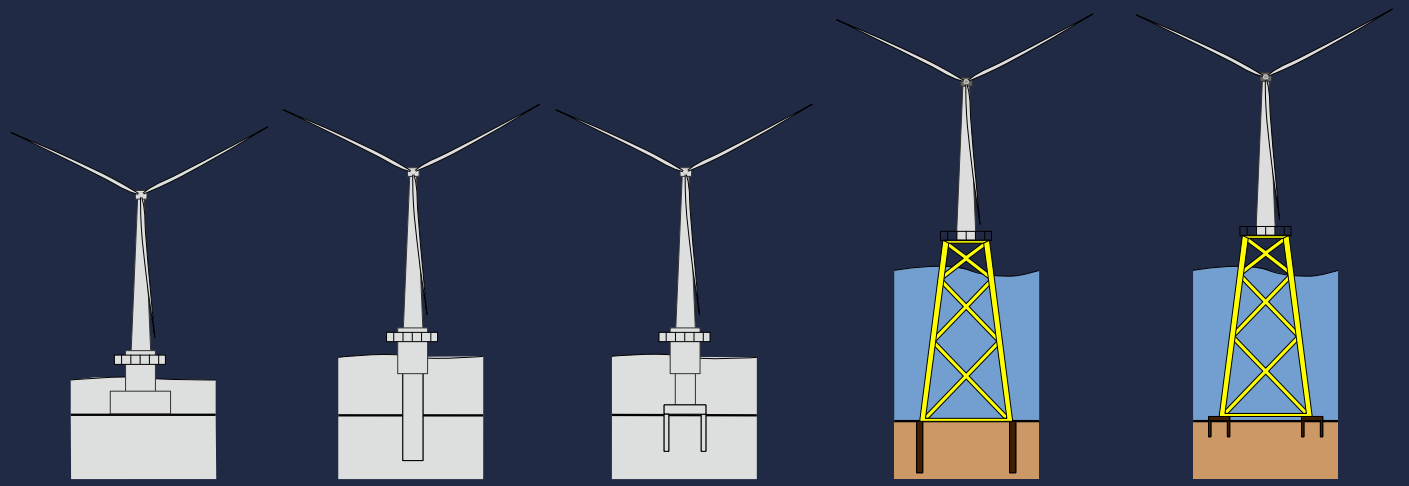

Floating

OWT environment and design

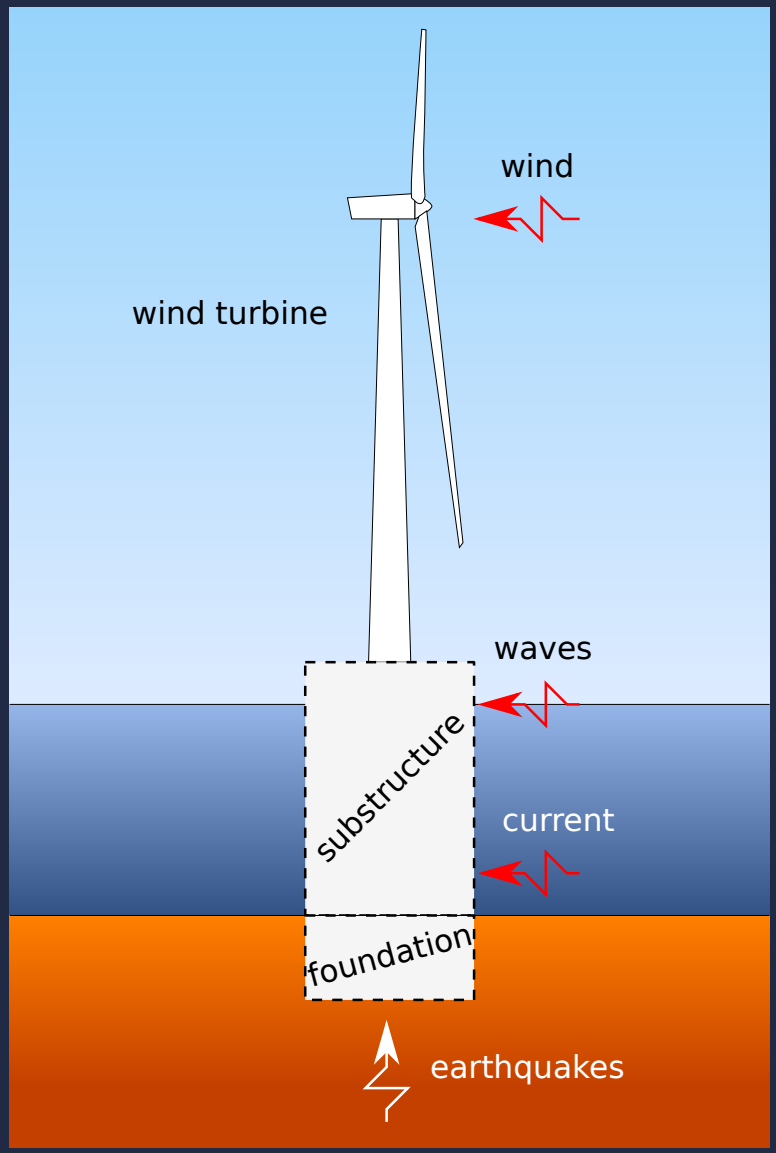

Figure: Challenging environment and design. Image source: D. Schroeder

Fundamental frequency challenge

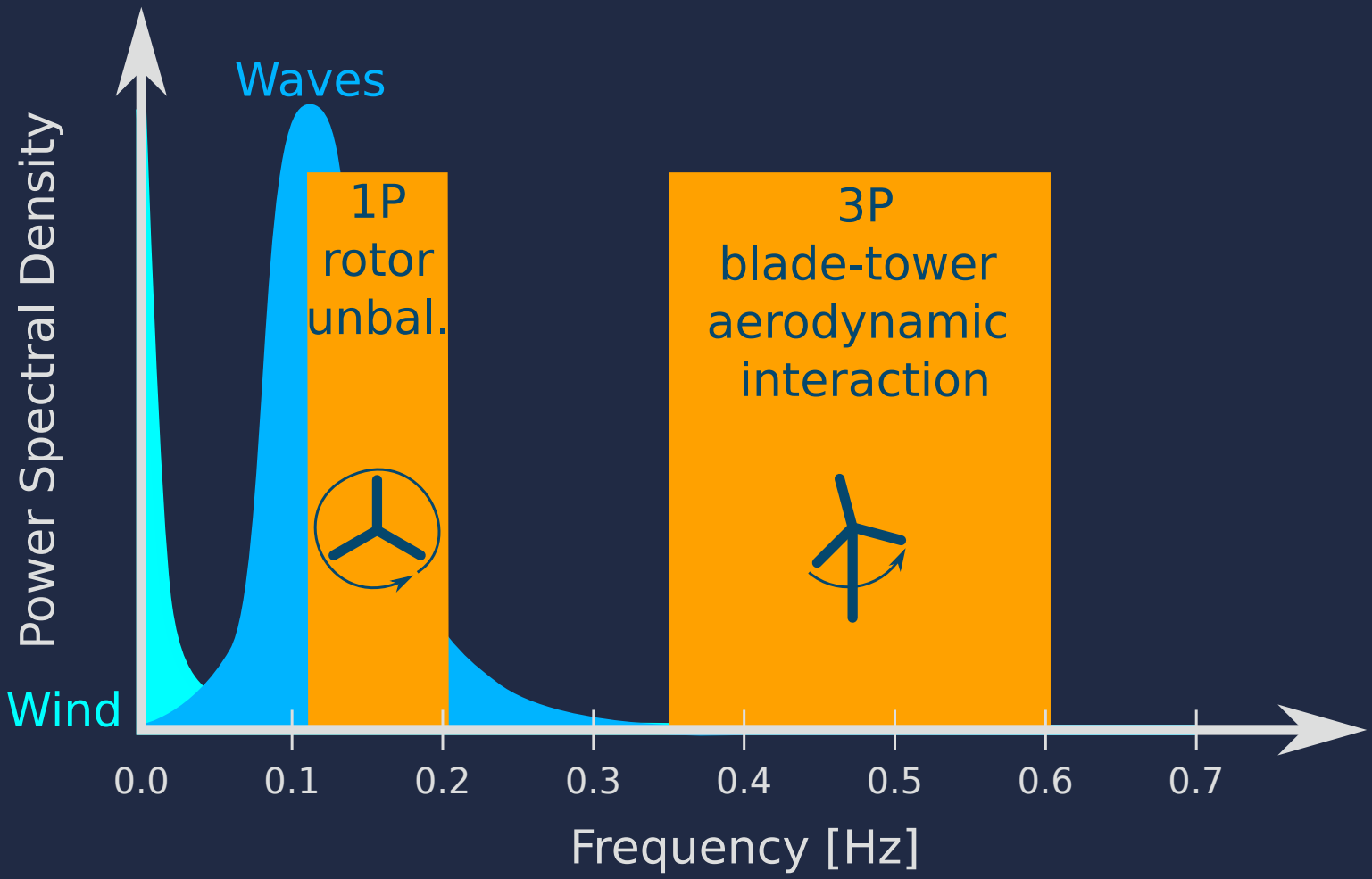

Figure: Dynamic loads and OWT fundamental frequency

Fundamental frequency challenge

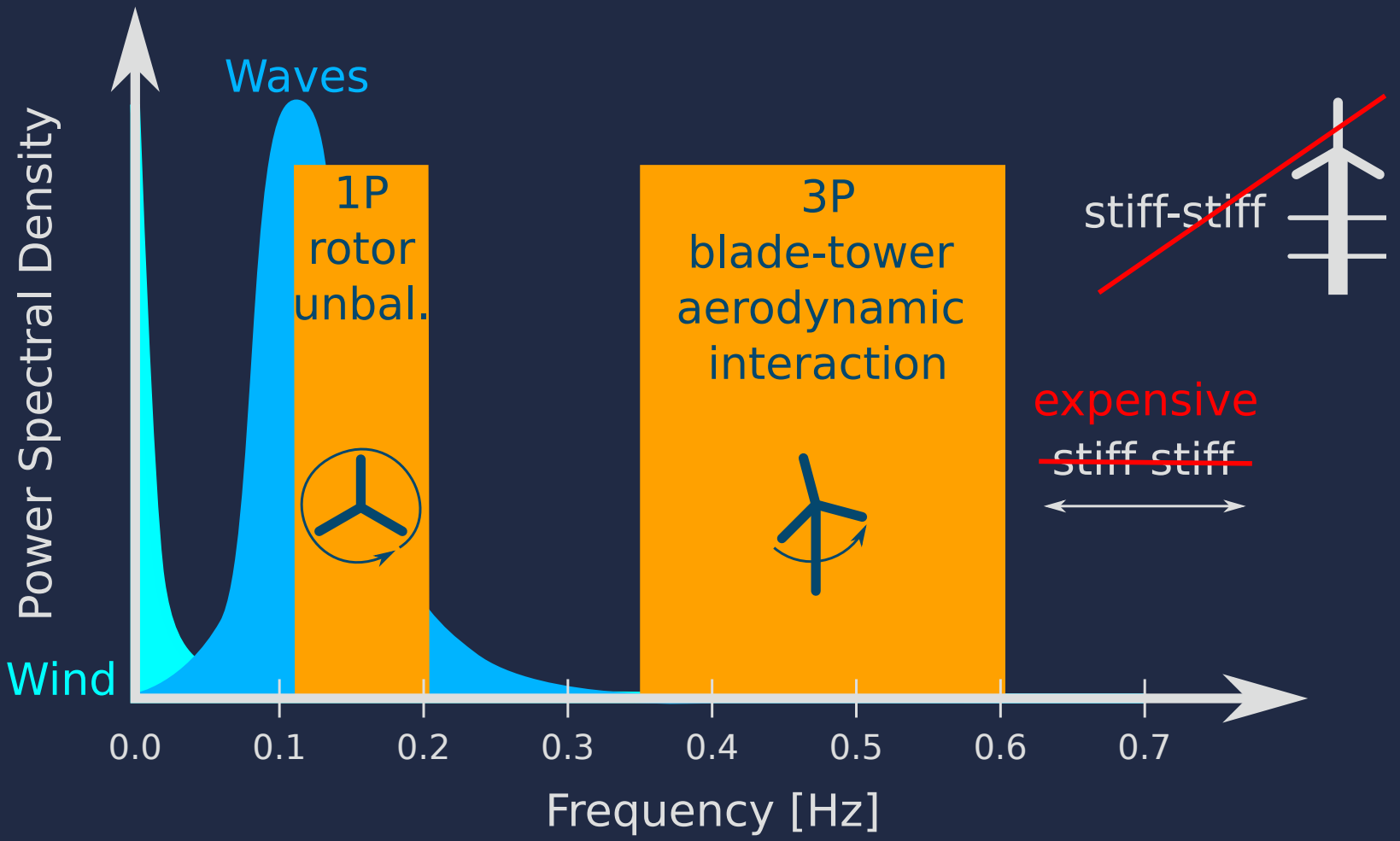

Figure: Dynamic loads and OWT fundamental frequency

Fundamental frequency challenge

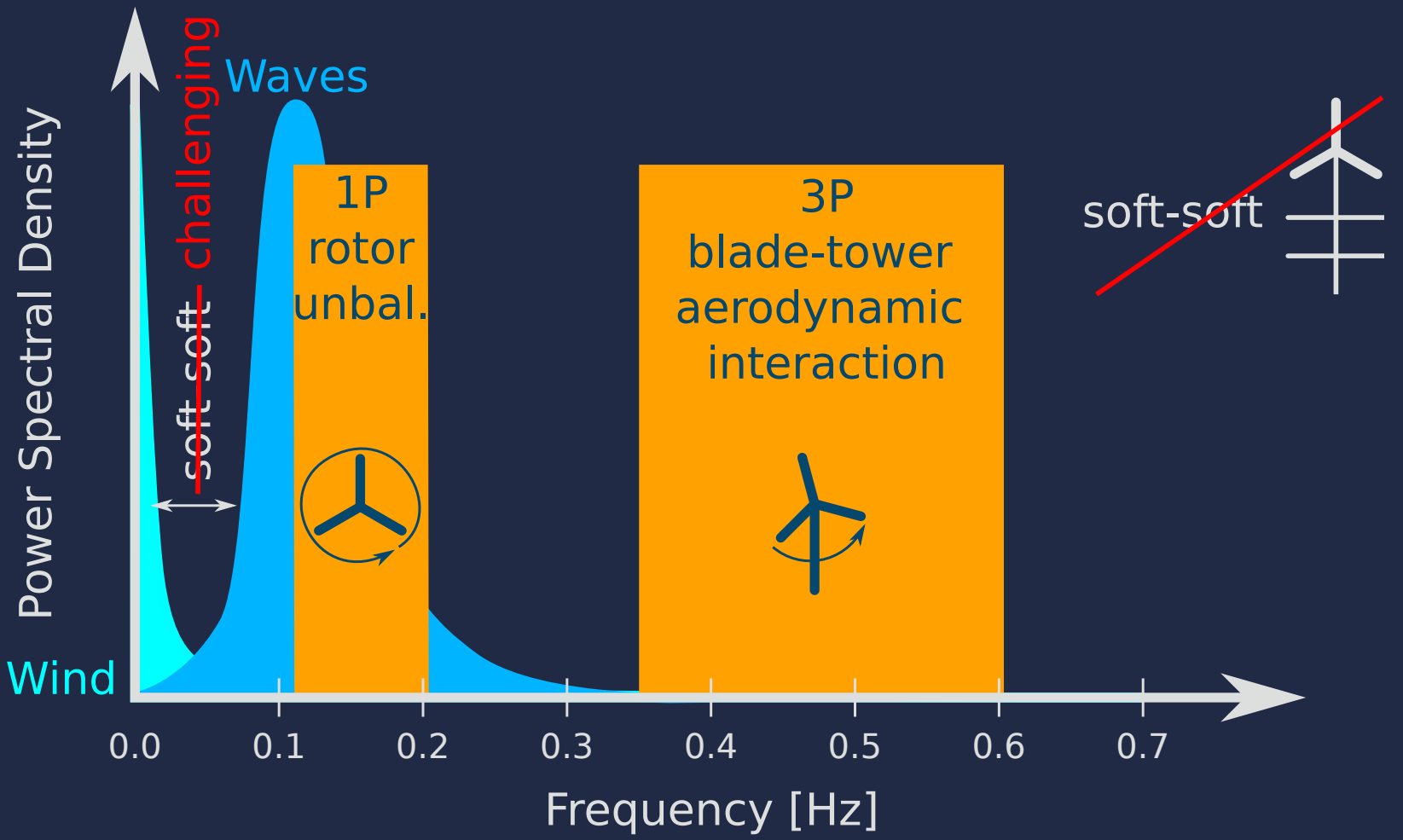

Figure: Dynamic loads and OWT fundamental frequency

Fundamental frequency challenge

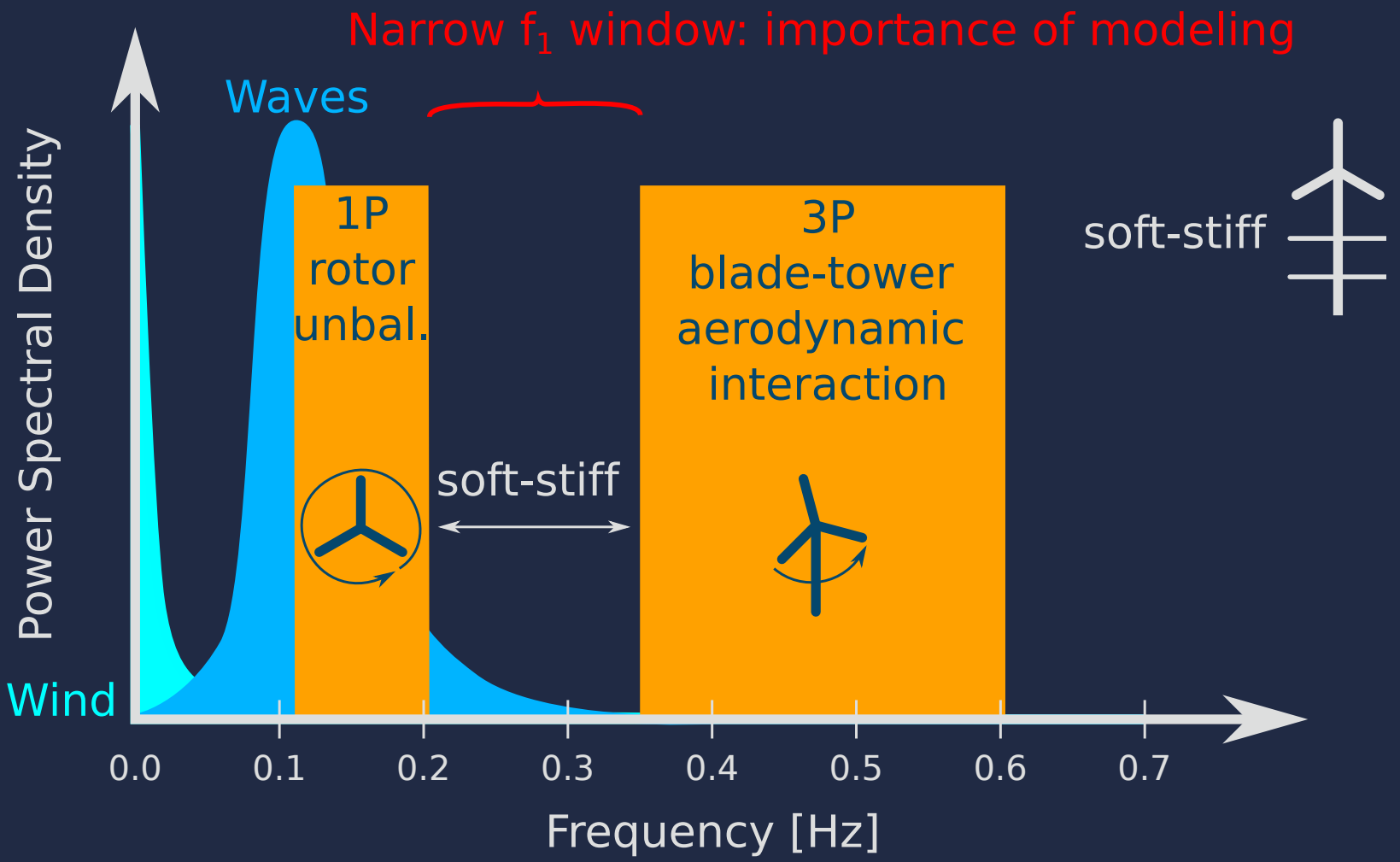

Figure: Dynamic loads and OWT fundamental frequency

OWT Soil-Structure Interaction (SSI) modeling

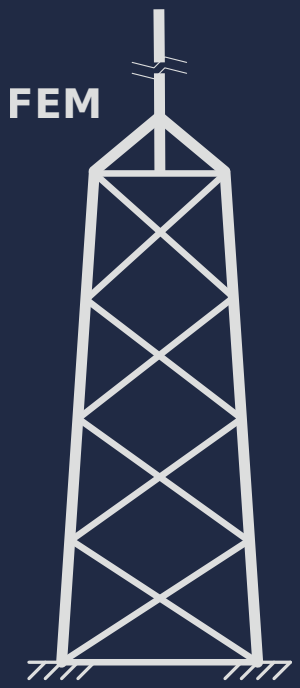

Rigid base

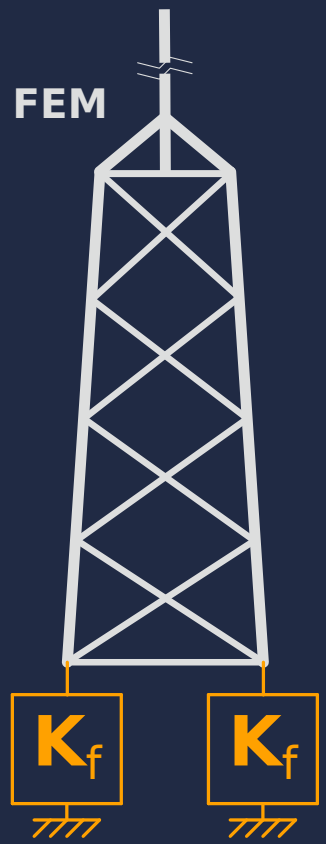

Flexible base **without** foundation interaction

No SSI

SSI

OWT Soil-Structure Interaction (SSI) modeling

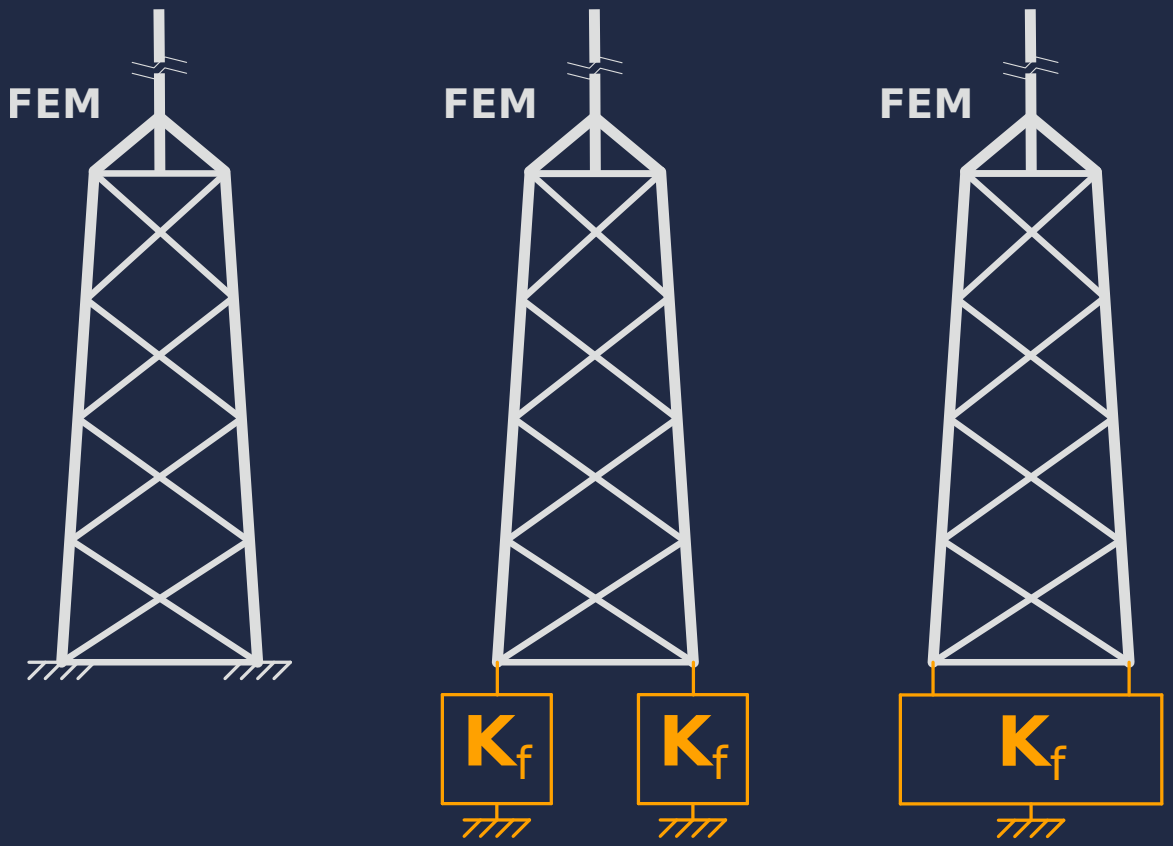

Rigid base

Flexible base **without** foundation interaction

Flexible base **with** foundation interaction

No SSI

SSI

OWT Soil-Structure Interaction (SSI) modeling

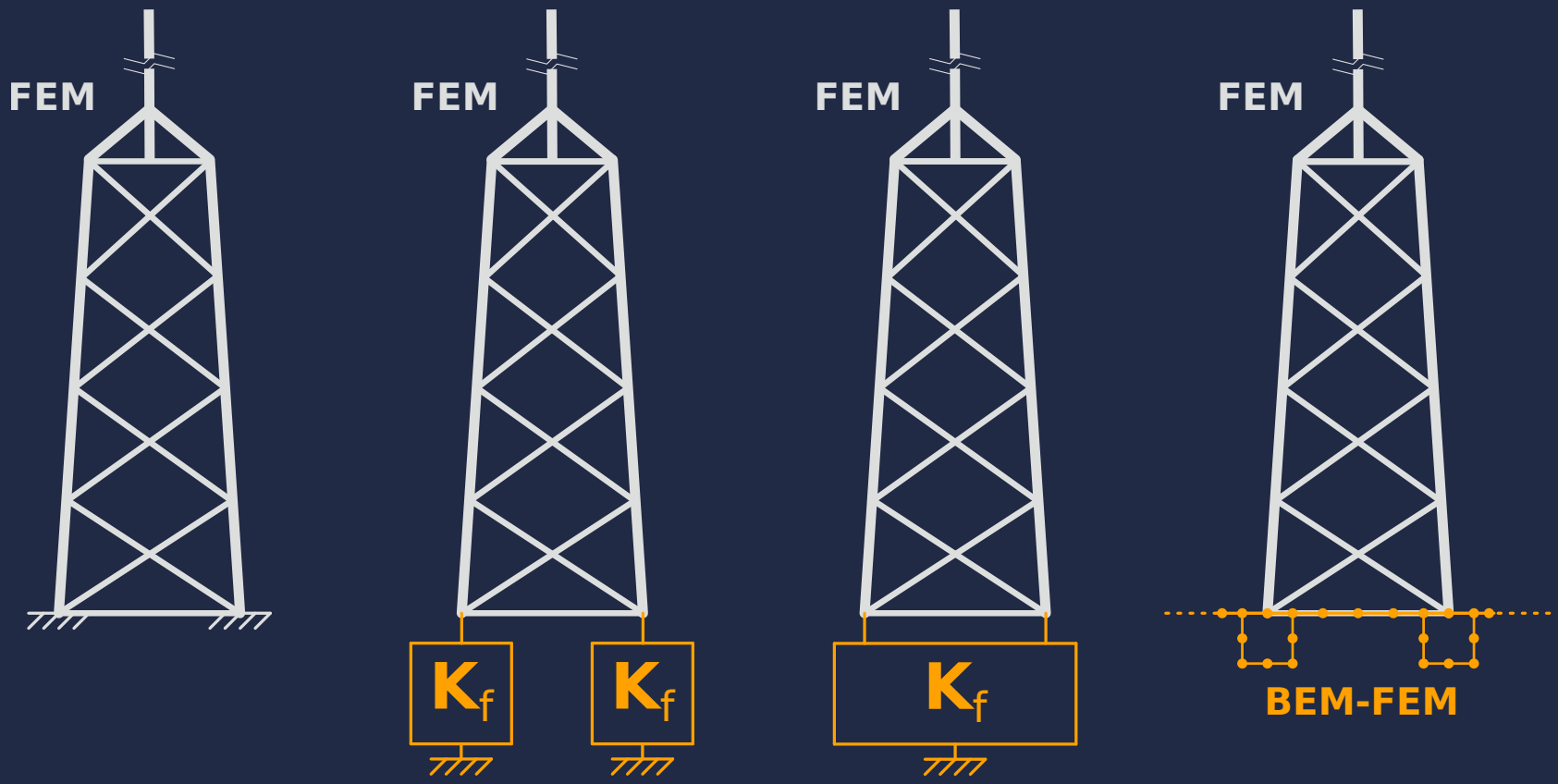

Rigid base

Flexible base **without** foundation interaction

Flexible base **with** foundation interaction

Direct model

No SSI

SSI

OWT Soil-Structure Interaction (SSI) modeling

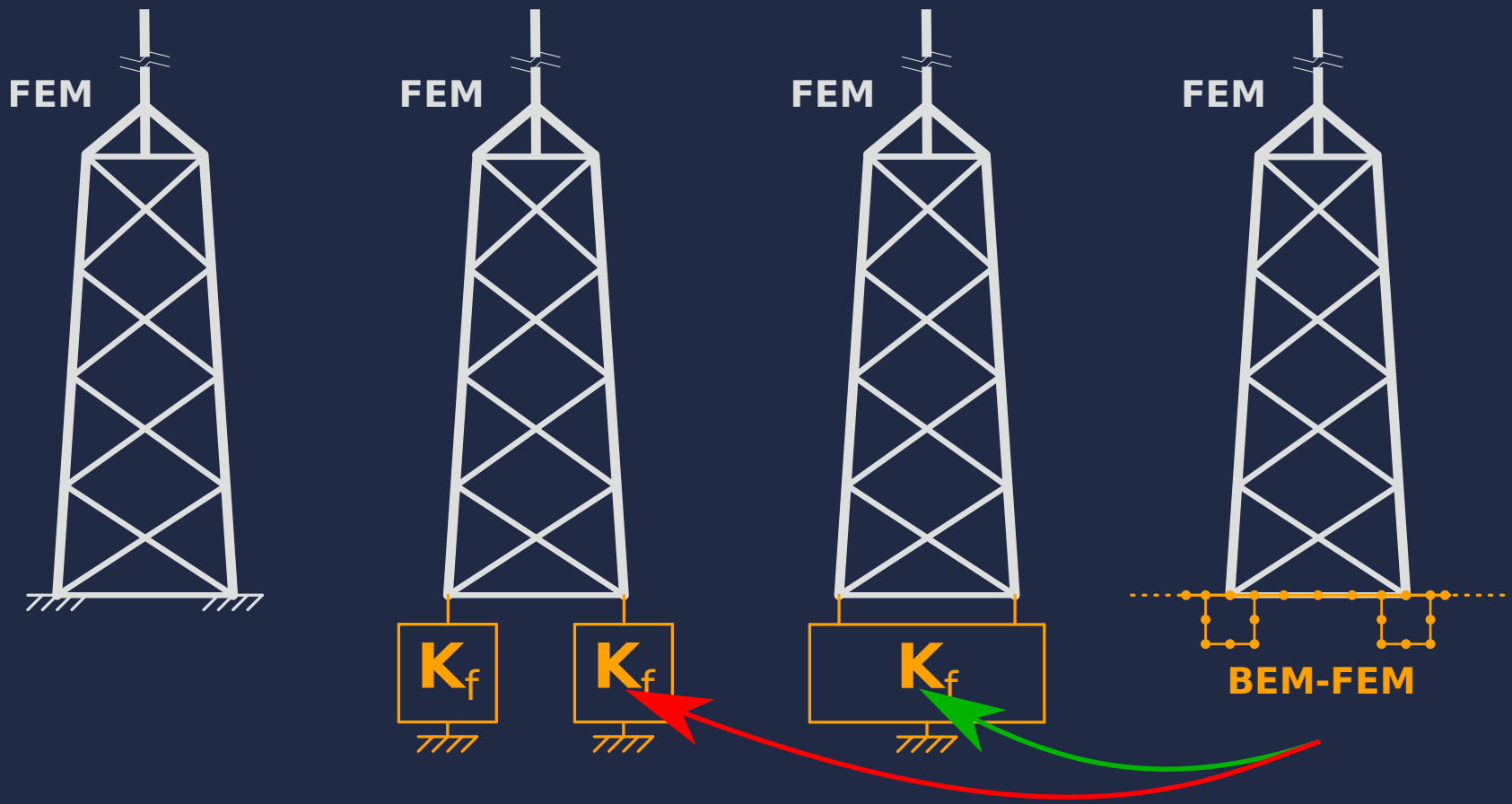

Rigid base

Flexible base **without** foundation interaction

Flexible base **with** foundation interaction

Direct model

No SSI

SSI

Modeling assumptions and aim

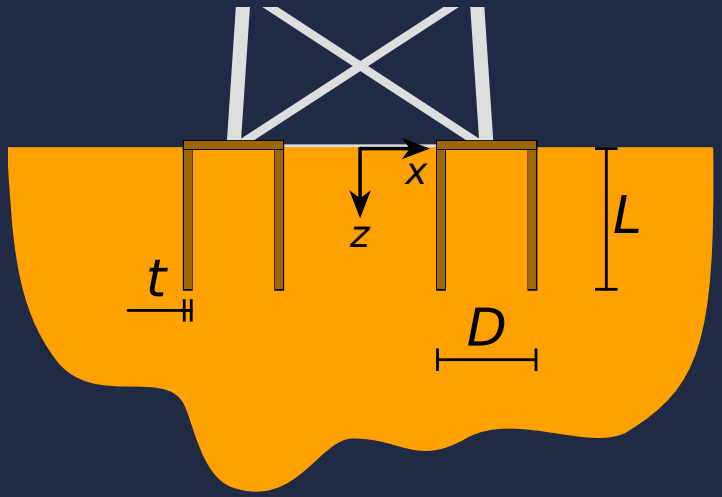

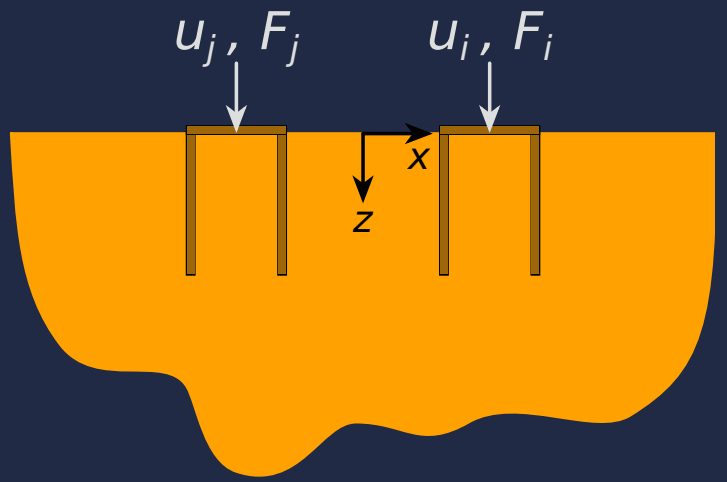

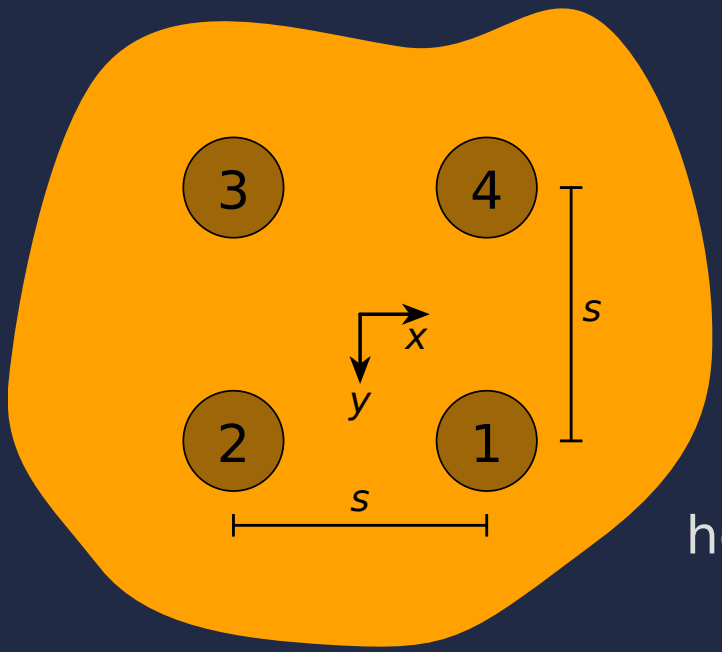

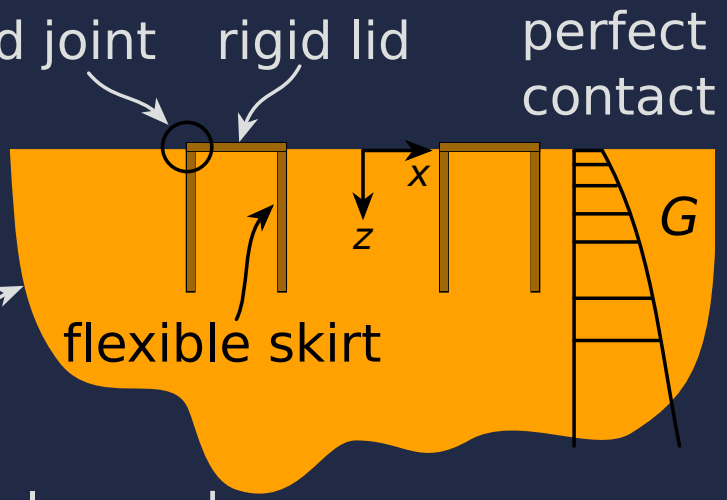

horizontally layered half-space

Outline

Vertical interaction

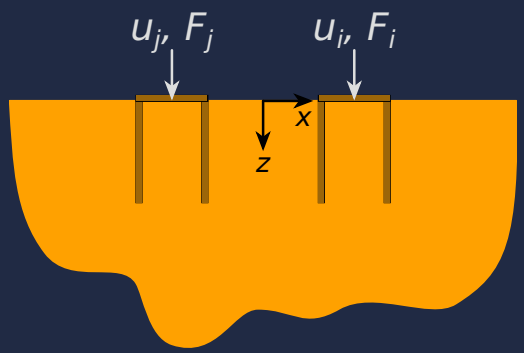

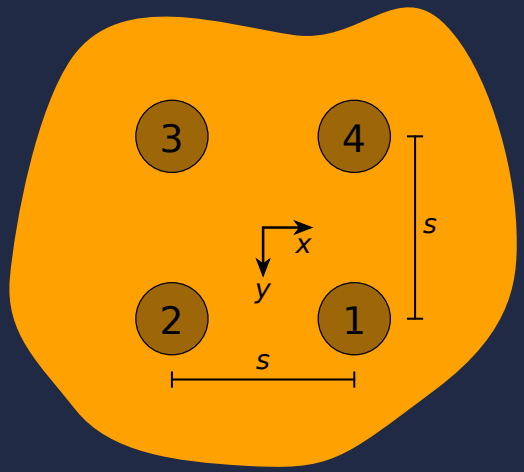

$$\begin{Bmatrix} F_1 \\ F_2 \\ F_3 \\ F_4 \end{Bmatrix} = \begin{bmatrix} K_{11} & K_{12} & K_{13} & K_{14} \\ & K_{22} & K_{23} & K_{24} \\ & & K_{33} & K_{34} \\ \text{sym.} & & & K_{44} \end{bmatrix} \begin{Bmatrix} u_1 \\ u_2 \\ u_3 \\ u_4 \end{Bmatrix}$$

Vertical interaction

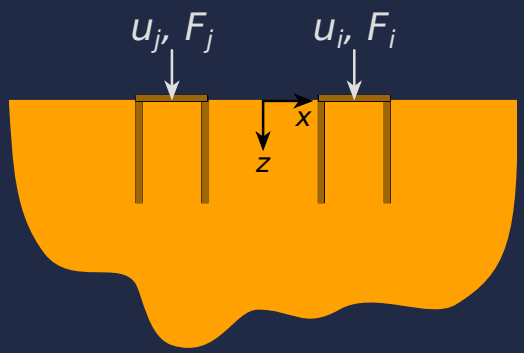

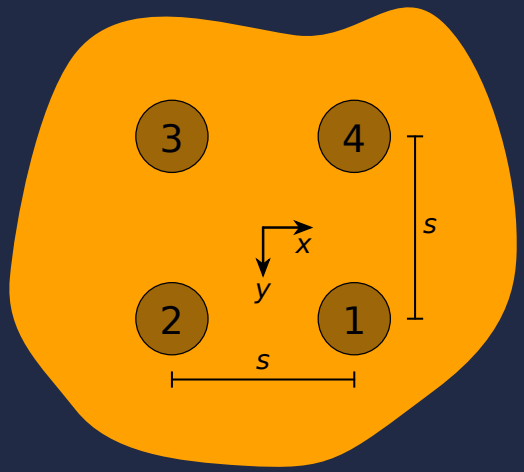

$$\begin{Bmatrix} F_1 \\ F_2 \\ F_3 \\ F_4 \end{Bmatrix} = \begin{bmatrix} K_{11} & K_{12} & K_{13} & K_{12} \\ & K_{11} & K_{12} & K_{13} \\ & & K_{11} & K_{12} \\ \text{sym.} & & & K_{11} \end{bmatrix} \begin{Bmatrix} u_1 \\ u_2 \\ u_3 \\ u_4 \end{Bmatrix}$$

K_{11} self

K_{12} side

K_{13} diagonal

Vertical interaction

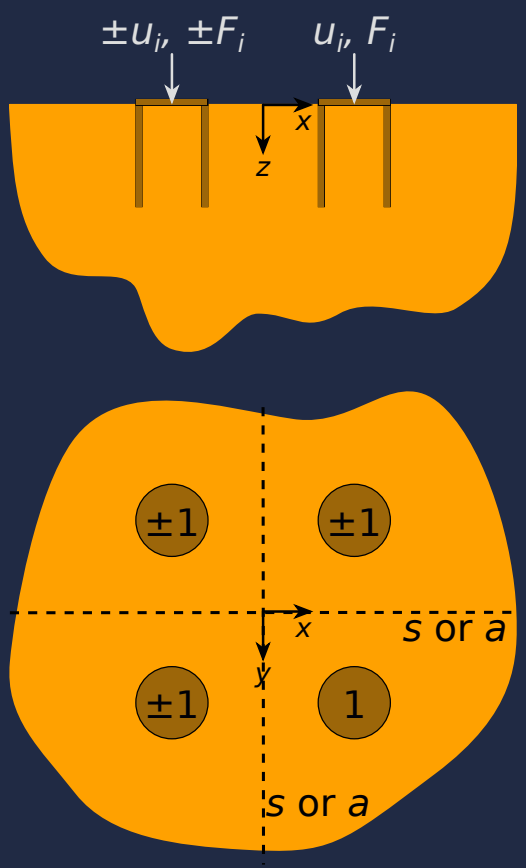

Exploiting the one-quarter symmetry:

- Plane zx: **s**ymmetry or **a**ntisymmetry
- Plane yz: **s**ymmetry or **a**ntisymmetry

Superposition of ss, sa, as (≡sa) and aa:

$$K_{11} = \frac{1}{4}\left(K_{ss} + 2K_{sa} + K_{aa}\right)$$

$$K_{12} = \frac{1}{4}\left(K_{ss} - K_{aa}\right)$$

$$K_{13} = \frac{1}{4}\left(K_{ss} - 2K_{sa} + K_{aa}\right)$$

Vertical interaction

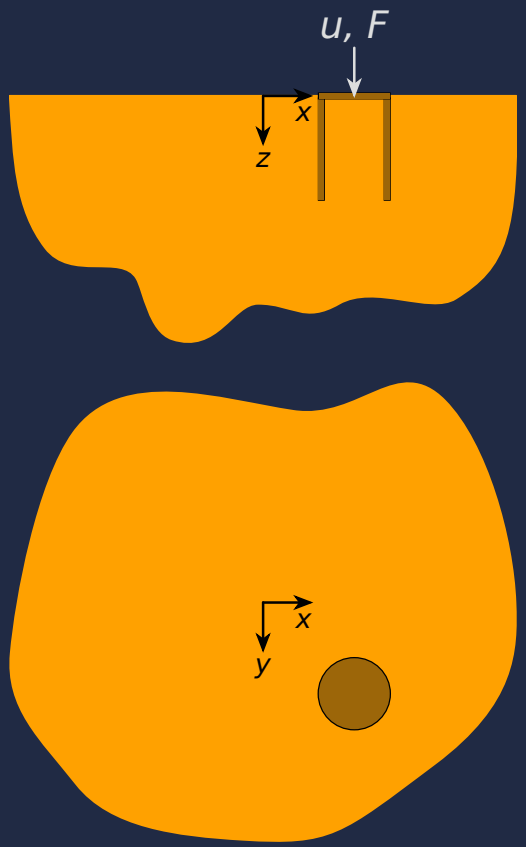

As $s \to \infty$:

$$K_{11} \to K_{\text{isolated}}$$
$$K_{12} \to 0$$
$$K_{13} \to 0$$

where K_{isolated} is the impedance of an isolated foundation.

BEM-FEM numerical approach (overview)

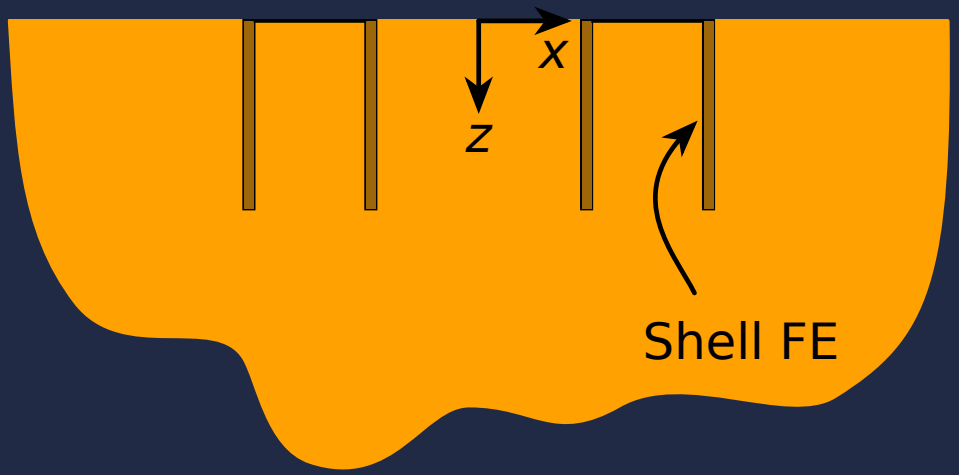

nodes with
5 $(u_x,u_y,u_z,\alpha,\beta)$
or
6 $(u_x,u_y,u_z,\theta_x,\theta_y,\theta_z)$
DOFs

- Skirts: Shell Finite Elements.
  - Shell degenerated from solid - MITC9[1]

1

2

BEM-FEM numerical approach (overview)

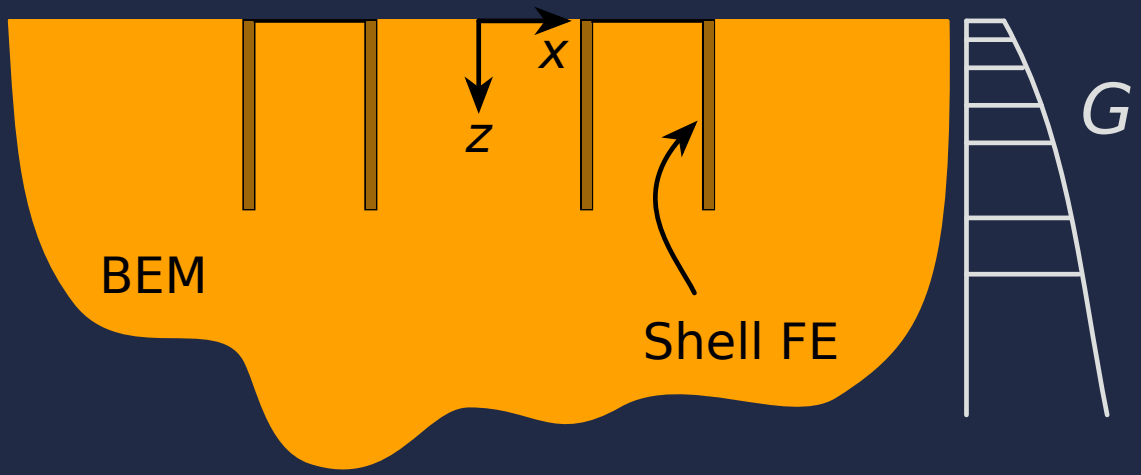

- Skirts: Shell Finite Elements.
  - Shell degenerated from solid - MITC9[1]
- Soil: Boundary Element Method.

[1] Bucalem & Bathe. Higher-order MITC general shell elements. Int J Num Meth Eng, 36, 1993.

[2]

BEM-FEM numerical approach (overview)

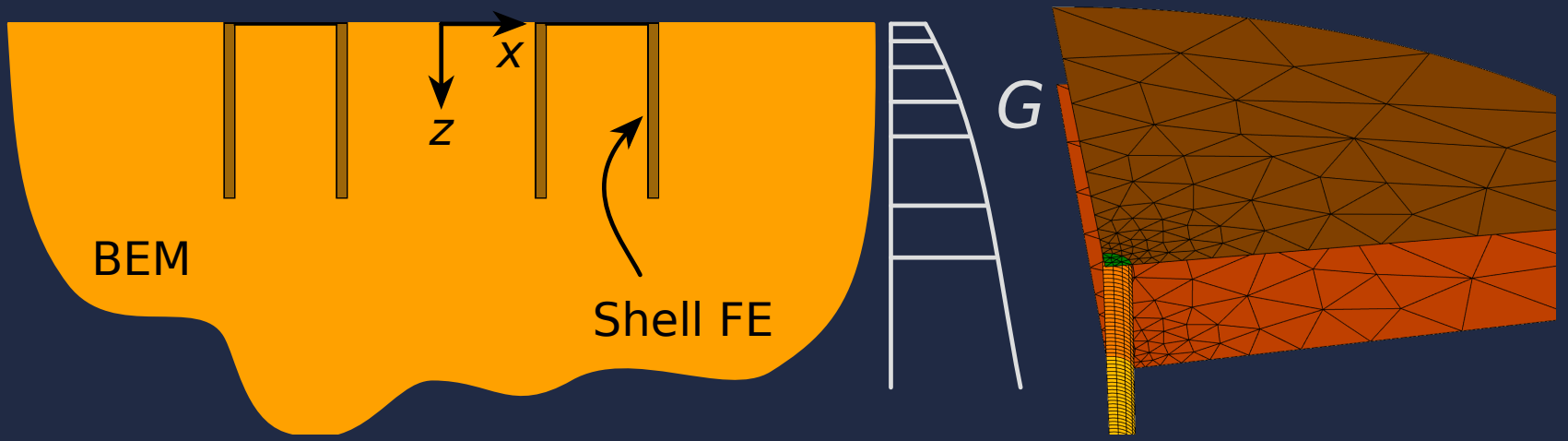

- Skirts: Shell Finite Elements.
  - Shell degenerated from solid - MITC9[1]
- Soil: Boundary Element Method.

[1] Bucalem & Bathe. Higher-order MITC general shell elements. Int J Num Meth Eng, 36, 1993.

[2]

BEM-FEM numerical approach (overview)

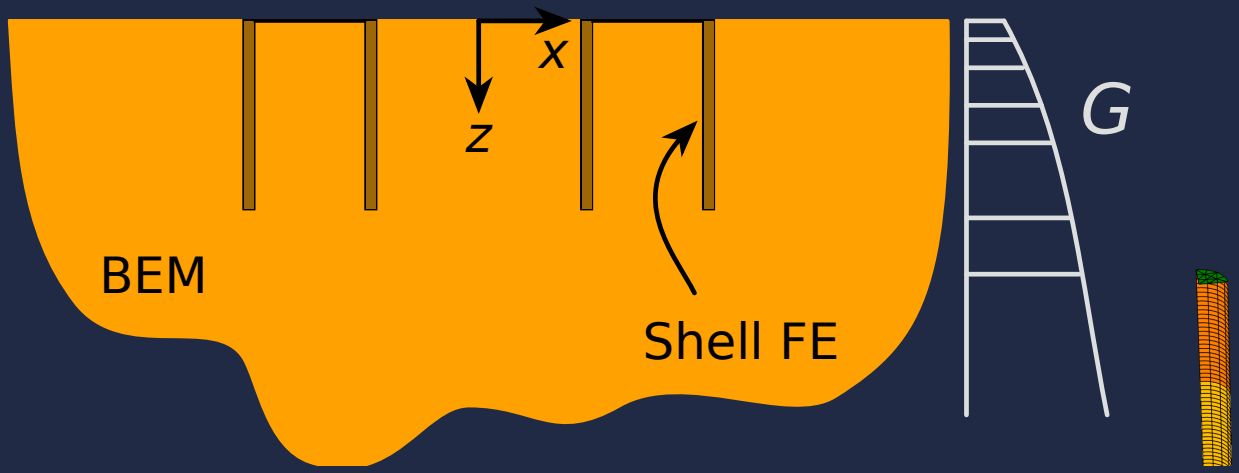

- Skirts: Shell Finite Elements.
  - Shell degenerated from solid - MITC9[1]
- Soil: Boundary Element Method.
  - Green's function for horizontally layered half-space[2]

---

[1] Bucalem & Bathe. Higher-order MITC general shell elements. Int J Num Meth Eng, 36, 1993.

[2] Pak & Guzina. Three-dimensional Green's functions for a multilayered half-space in displacement potentials. J Eng Mech, 128, 2002.

BEM-FEM numerical approach (some details)

Displacement Boundary Integral Equation:

$$c^i_{lk} u^i_k + \int_{\Gamma_{\text{lid}}} t^*_{lk} u_k \, \mathrm{d}\Gamma = \int_{\Gamma_{\text{lid}}} u^*_{lk} t_k \, \mathrm{d}\Gamma + \int_{\Pi_{\text{skirt}}} u^*_{lk} b_k \, \mathrm{d}\Pi \Rightarrow \mathbf{Hu} = \mathbf{Gt} + \mathbf{G}_b\mathbf{b}$$

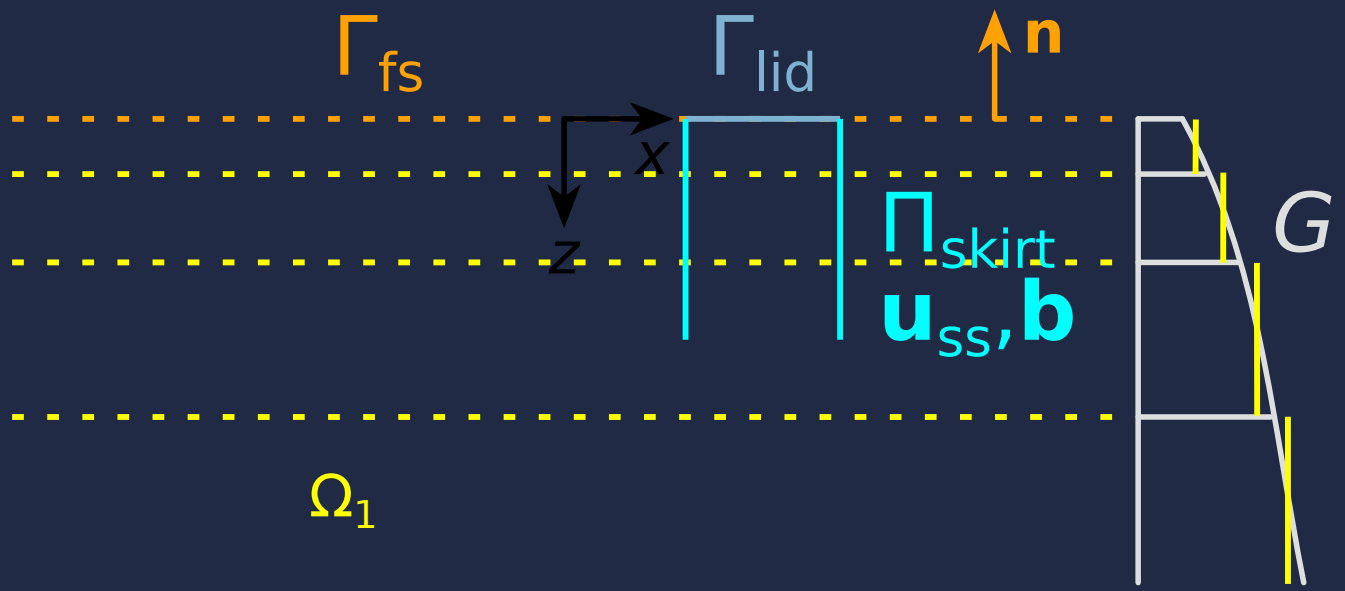

BEM-FEM numerical approach (some details)

Displacement Boundary Integral Equation:

$$c_{lk}^{i} u_k^i + \int_{\Gamma_{\text{lid}}} t_{lk}^{*} u_k \, \mathrm{d}\Gamma = \int_{\Gamma_{\text{lid}}} u_{lk}^{*} t_k \, \mathrm{d}\Gamma + \int_{\Pi_{\text{skirt}}} u_{lk}^{*} b_k \, \mathrm{d}\Pi \Rightarrow \mathbf{Hu} = \mathbf{Gt} + \mathbf{G}_b\mathbf{b}$$

Shell finite element equilibrium equation (element level):

$$\Omega_{\text{skirt}} : \ \mathbf{K}^{(e)}\mathbf{a}^{(e)} - \mathbf{Q}^{(e)}\mathbf{f}^{(e)} = \mathbf{q}^{(e)}$$

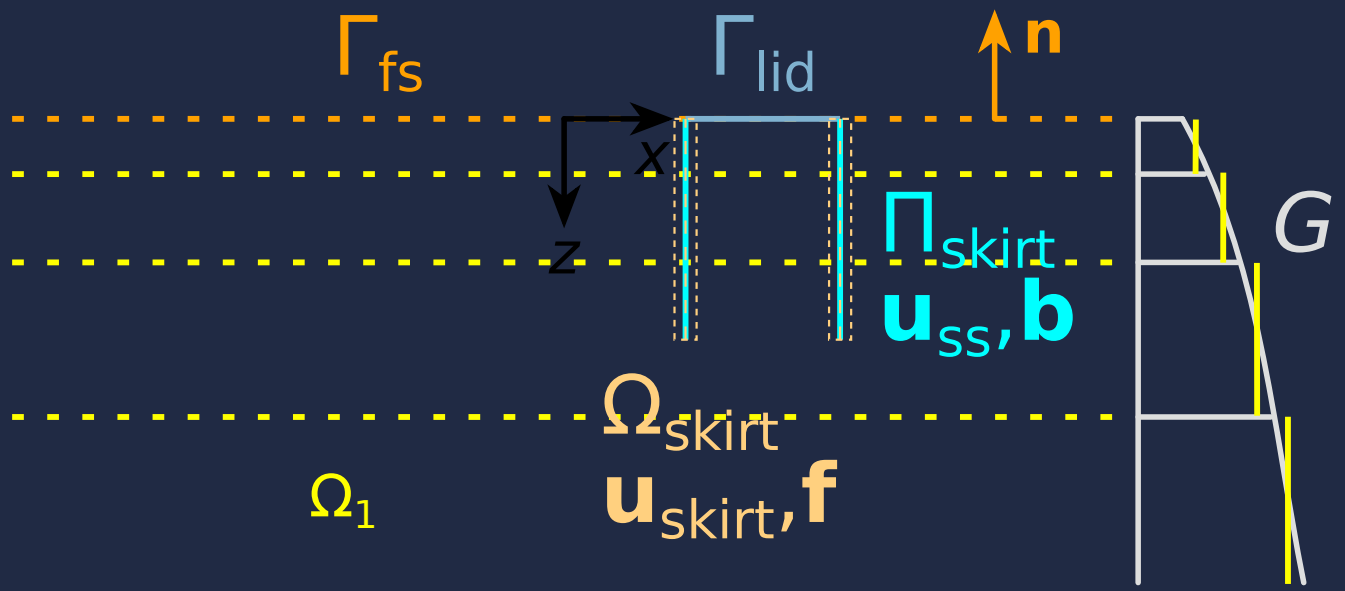

BEM-FEM numerical approach (some details)

Displacement Boundary Integral Equation:

$$c_{lk}^{i} u_k^i + \int_{\Gamma_{\text{lid}}} t_{lk}^{*} u_k \, \mathrm{d}\Gamma = \int_{\Gamma_{\text{lid}}} u_{lk}^{*} t_k \, \mathrm{d}\Gamma + \int_{\Pi_{\text{skirt}}} u_{lk}^{*} b_k \, \mathrm{d}\Pi \Rightarrow \mathbf{Hu} = \mathbf{Gt} + \mathbf{G}_b\mathbf{b}$$

Shell finite element equilibrium equation (element level):

$$\Omega_{\text{skirt}} : \ \mathbf{K}^{(e)}\mathbf{a}^{(e)} - \mathbf{Q}^{(e)}\mathbf{f}^{(e)} = \mathbf{q}^{(e)}$$

Perfect contact: compatibility $\mathbf{u}_{\text{ss}} = \mathbf{u}_{\text{skirt}}$ and equilibrium $\mathbf{b} + \mathbf{f} = \mathbf{0}$.

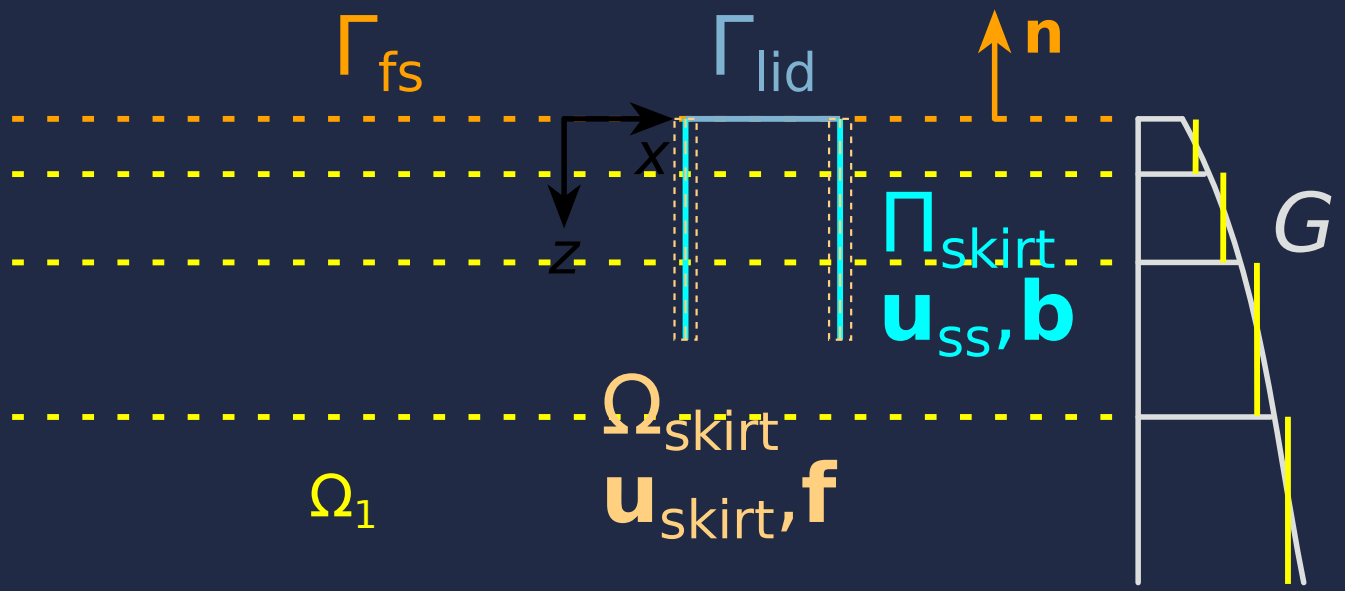

Horizontally Layered Half-space Green's function

- Regularization of the integral:

$$\oint_{\Gamma_{\text{lid}}} t^*_{lk} u_k \, \mathrm{d}\Gamma = \int_{\Gamma_{\text{lid}}} [t^*_{lk} - (t^*_{lk})_{\text{Mindlin}}] \, u_k \, \mathrm{d}\Gamma + \oint_{\Gamma_{\text{lid}}} (t^*_{lk})_{\text{Mindlin}} \, u_k \, \mathrm{d}\Gamma$$

  where $(t^*_{lk})_{\text{Mindlin}}$ are tractions of the homogeneous half-space GF in statics.

Horizontally Layered Half-space Green's function

- Regularization of the integral:

$$\oint_{\Gamma_{\text{lid}}} t^*_{lk} u_k \, \mathrm{d}\Gamma = \int_{\Gamma_{\text{lid}}} [t^*_{lk} - (t^*_{lk})_{\text{Mindlin}}] \, u_k \, \mathrm{d}\Gamma + \oint_{\Gamma_{\text{lid}}} (t^*_{lk})_{\text{Mindlin}} \, u_k \, \mathrm{d}\Gamma$$

  where $(t^*_{lk})_{\text{Mindlin}}$ are tractions of the homogeneous half-space GF in statics.

- Overall computational cost – a trade-off between:
  - DOF reduction: smaller LSE
  - HLGF cost $>>$ fundamental solution cost: costly LSE

Horizontally Layered Half-space Green's function

- Regularization of the integral:

$$\oint_{\Gamma_{\text{lid}}} t^*_{lk} u_k \, \mathrm{d}\Gamma = \int_{\Gamma_{\text{lid}}} [t^*_{lk} - (t^*_{lk})_{\text{Mindlin}}] \, u_k \, \mathrm{d}\Gamma + \oint_{\Gamma_{\text{lid}}} (t^*_{lk})_{\text{Mindlin}} \, u_k \, \mathrm{d}\Gamma$$

  where $(t^*_{lk})_{\text{Mindlin}}$ are tractions of the homogeneous half-space GF in statics.

- Overall computational cost – a trade-off between:
  - DOF reduction: smaller LSE
  - HLGF cost $>>$ fundamental solution cost: costly LSE
- Develop strategies to reduce the number of HLGF evaluations.

Horizontally Layered Half-space Green's function

a Build a database of HLGF evaluations $(u^*_{lk},\ \sigma^*_{lkj})$ based on:

- Axial symmetry: database indexed by (z_s, z_o, r)

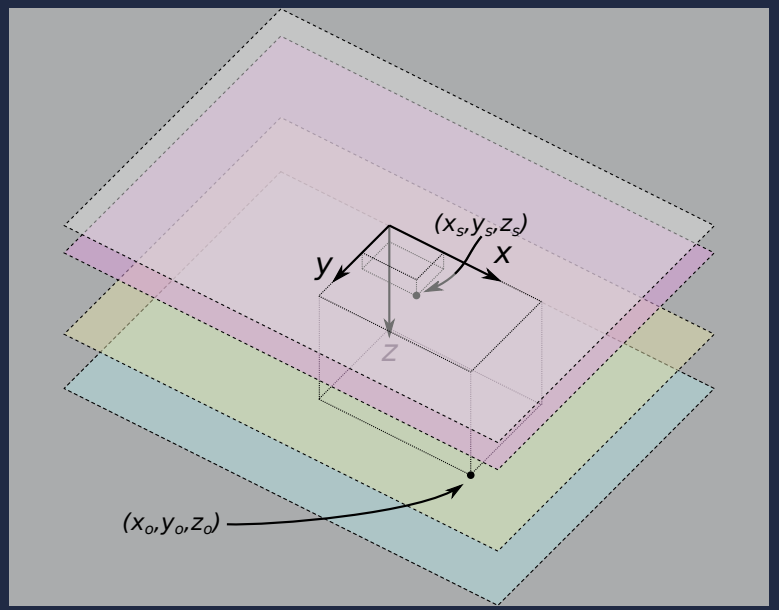

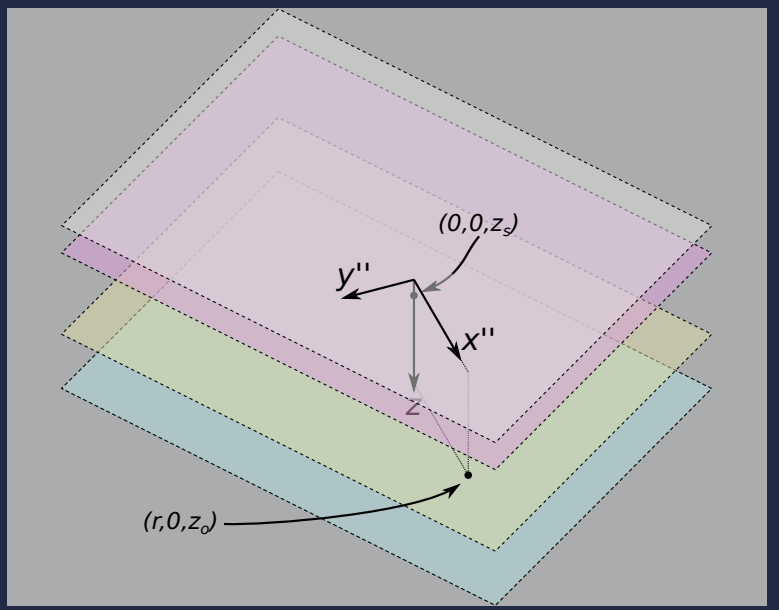

b Mesh regularity

BEM-FEM model

Quadratic 9-node elements

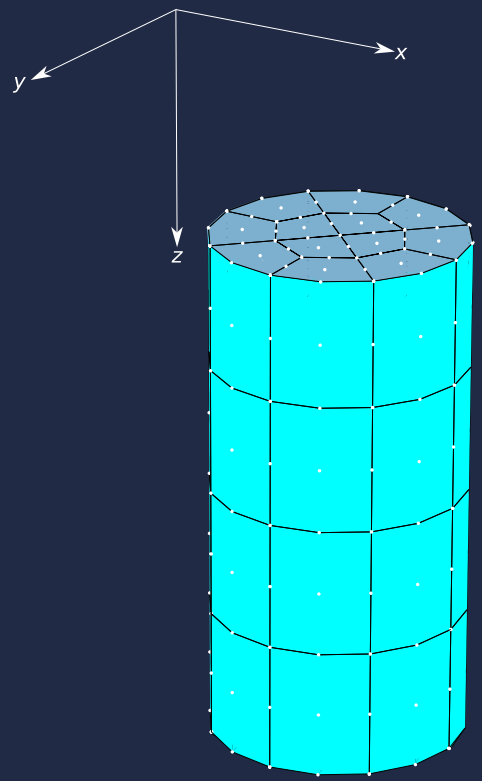

Figure: Example mesh: $L/D = 2$, $s/D = 4$

BEM-FEM model: lid

Quadratic 9-node boundary elements

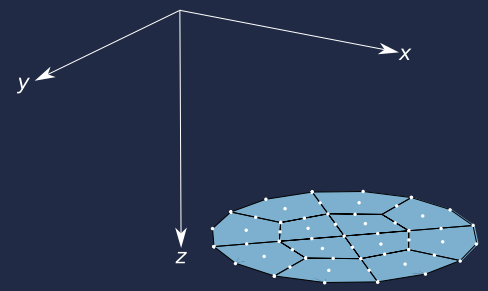

BC:

$$\mathbf{u} = (0, 0, 1)$$

When solved:

$$K^{(lid)} = \int_{\Gamma_{\text{lid}}} t_z \, \mathrm{d}\Gamma$$

Figure: Example mesh: $L/D = 2$, $s/D = 4$

BEM-FEM model: skirt

Quadratic 9-node shell finite elements (MITC9)

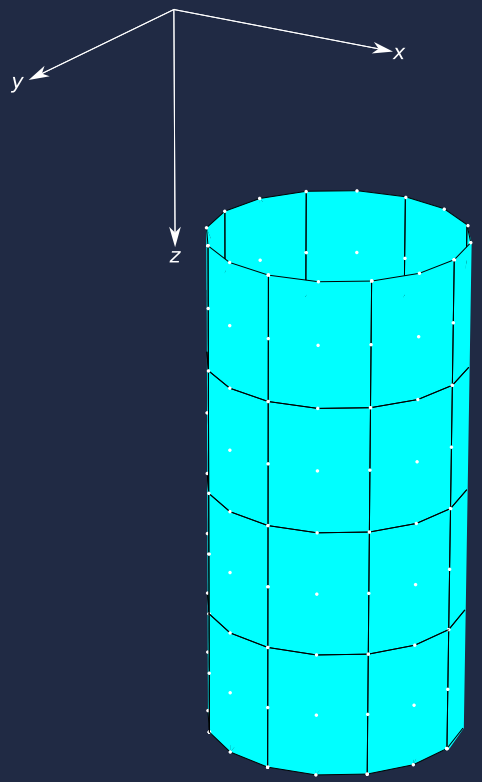

Figure: Example mesh: $L/D = 2$, $s/D = 4$

BC (top nodes):

$$\begin{Bmatrix} u_x \\ u_y \\ u_z \\ \theta_x \\ \theta_y \\ \theta_z \end{Bmatrix} = \begin{Bmatrix} 0 \\ 0 \\ 1 \\ 0 \\ 0 \\ 0 \end{Bmatrix}$$

When solved:

$$K^{(skirt)} = \sum_{\text{top nodes}} F_z^{(i)}$$

BEM-FEM model: soil-skirt interface

Quadratic 9-node BEM body load surface elements

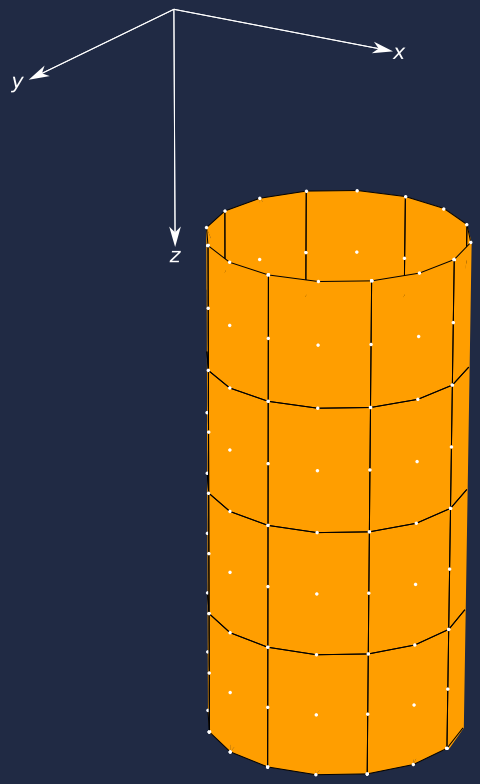

Figure: Example mesh: $L/D = 2$, $s/D = 4$

Perfect contact conditions:

$$\mathbf{u}_{\mathrm{ss}} = \mathbf{u}_{\mathrm{skirt}}$$

$$\mathbf{b}_{\mathrm{ss}} + \mathbf{f}_{\mathrm{skirt}} = \mathbf{0}$$

Outline

Cases: geometry

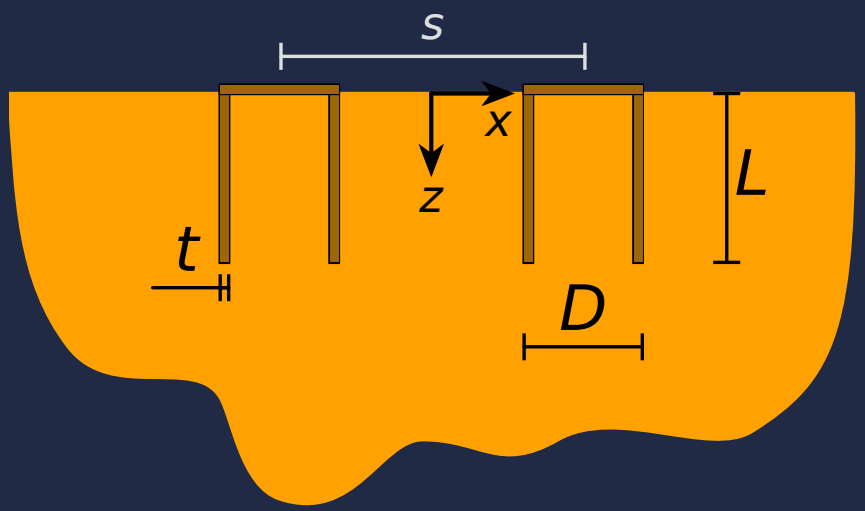

- Skirt thickness to diameter ratio: $\frac{t}{D} = 0.02$
- Depth to diameter ratios: $\frac{L}{D} = \{1, 2, 4\}$
- Spacing to diameter ratios: $\frac{s}{D} = \{2, 4, 8\}$

Cases: material properties

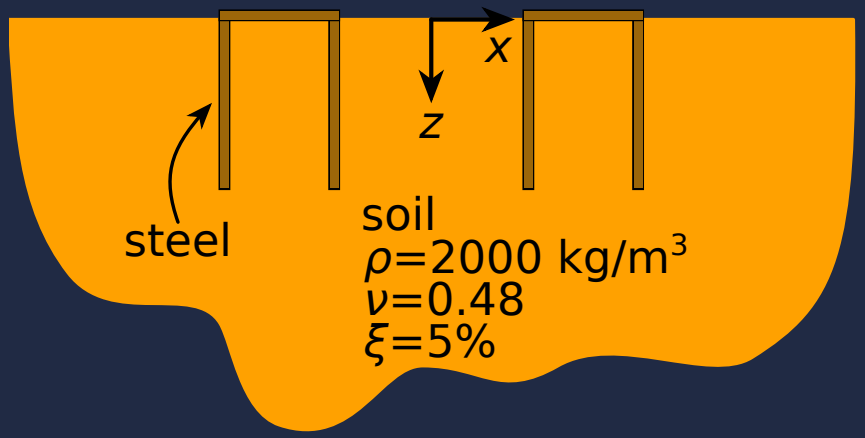

Cases: material properties

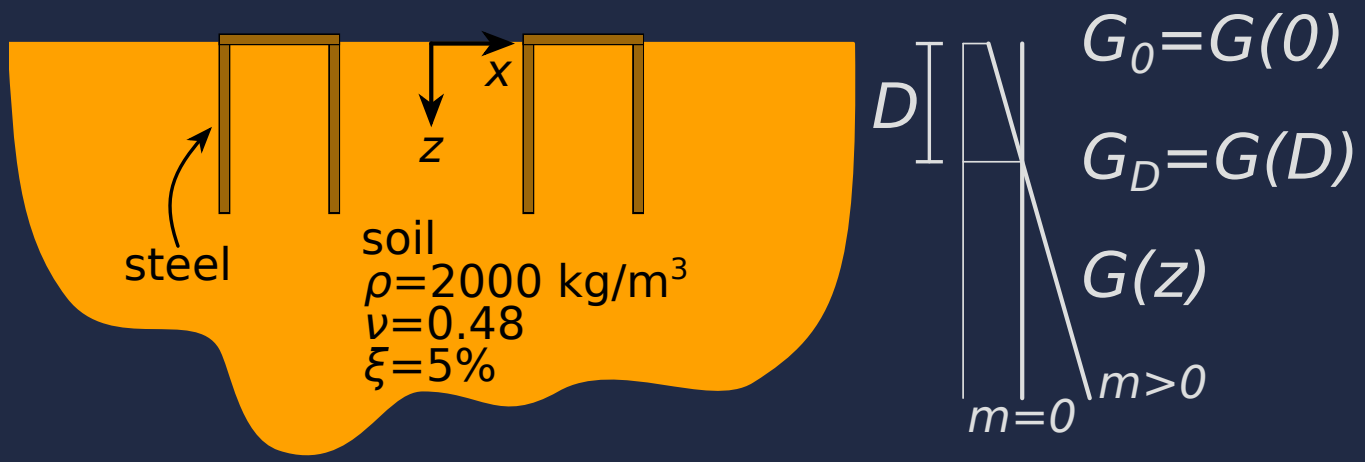

- Gibson soil: $G(z) = G_0 \left(1 + m\frac{z}{D}\right)$
  - $m = \frac{G_D}{G_0} - 1 = \{0, 0.2, 0.4\}$
  - $\frac{G_D}{G_0} = \{1, 1.2, 1.4\}$

Cases: material properties

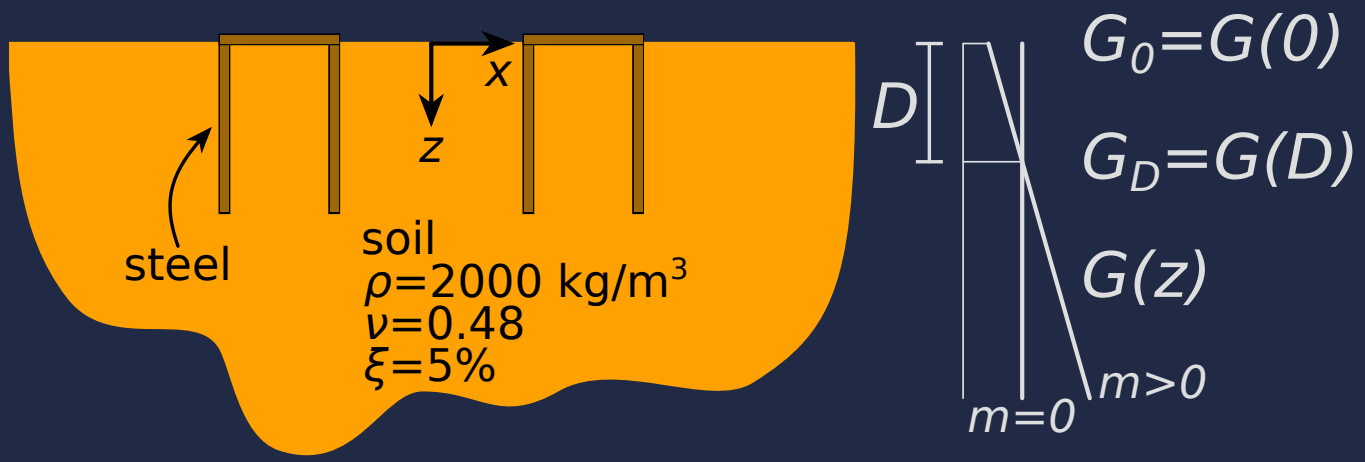

- Gibson soil: $G(z) = G_0 \left(1 + m\frac{z}{D}\right)$
  - $m = \dfrac{G_D}{G_0} - 1 = \{0, 0.2, 0.4\}$
  - $\dfrac{G_D}{G_0} = \{1, 1.2, 1.4\}$
- Skirt-soil stiffness ratio: $J = \dfrac{G_{\mathrm{st}}}{G_D}\dfrac{t}{D} = \{10, 100, 1000\}$

Cases: frequencies

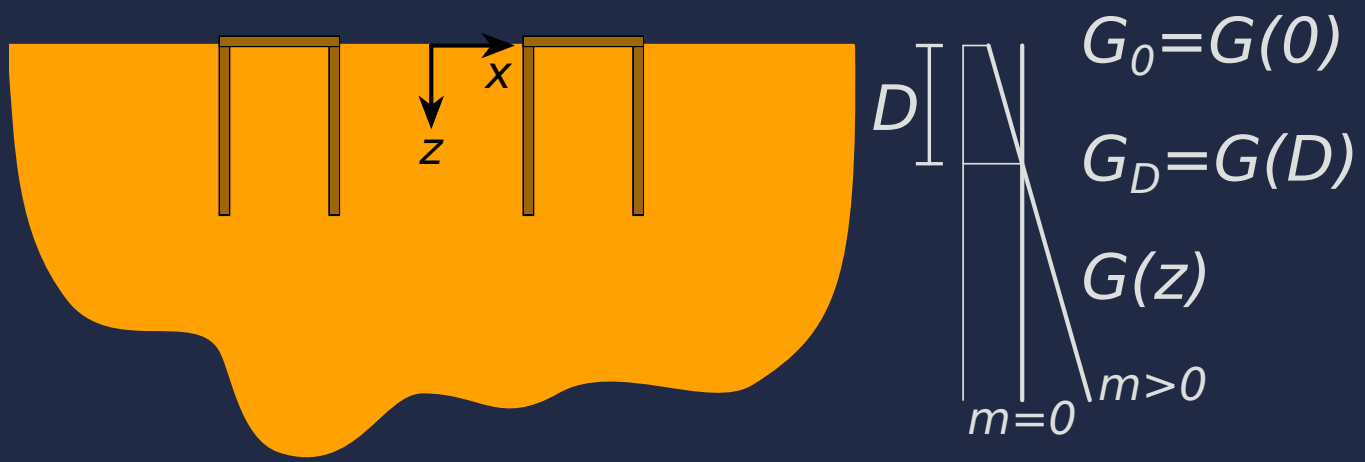

- Dimensionless frequency: $a_0 = \dfrac{D}{\lambda_{s,D}} = \dfrac{f\ D}{c_{s,D}}$

Cases: frequencies

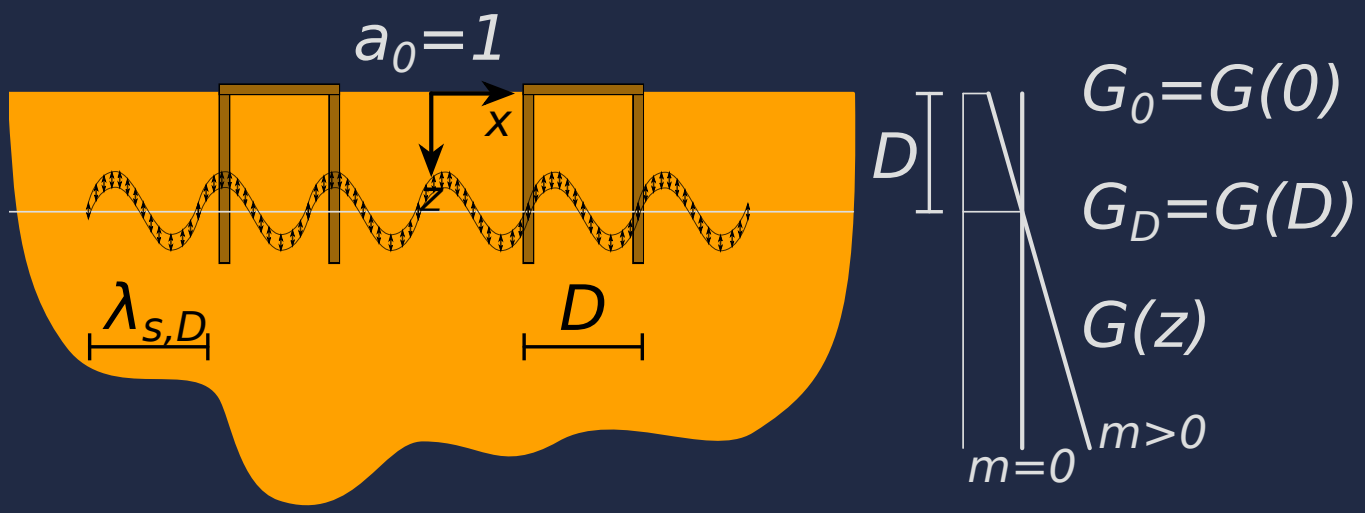

- Dimensionless frequency: $a_0 = \dfrac{D}{\lambda_{s,D}} = \dfrac{f\ D}{c_{s,D}}$

Cases: frequencies

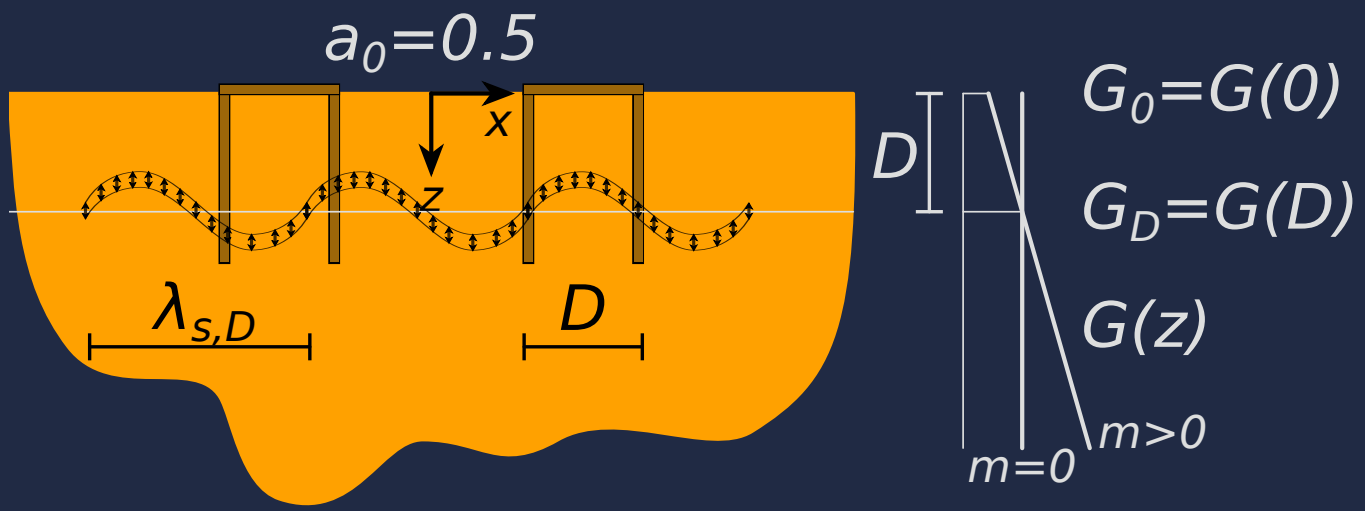

- Dimensionless frequency: $a_0 = \dfrac{D}{\lambda_{s,D}} = \dfrac{f\ D}{c_{s,D}} = (0, 0.5]$

K_{SS} vs L/D vs s/D, $J = 100$, homogeneous soil

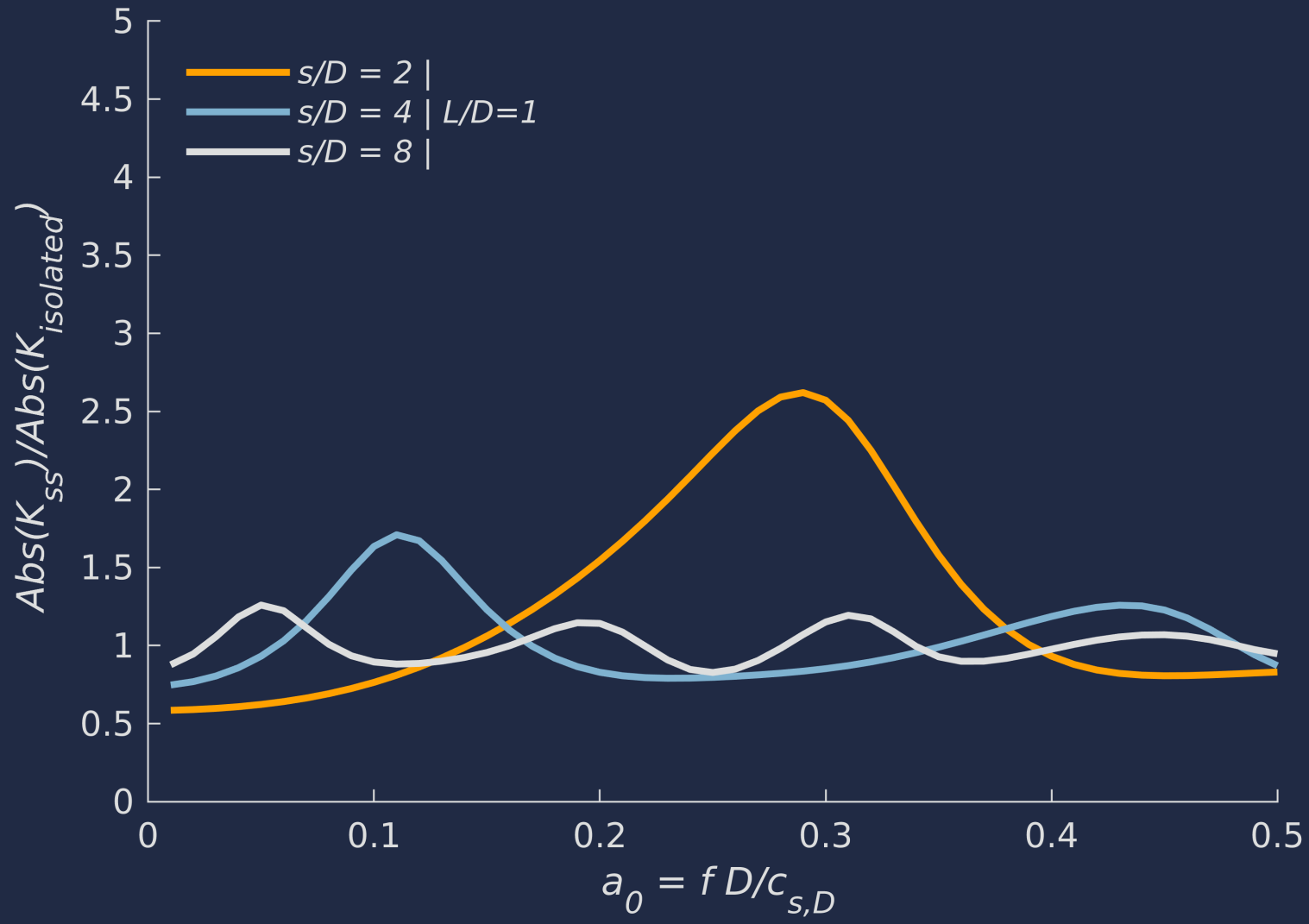

K_{SS} vs L/D vs s/D, $J = 100$, homogeneous soil

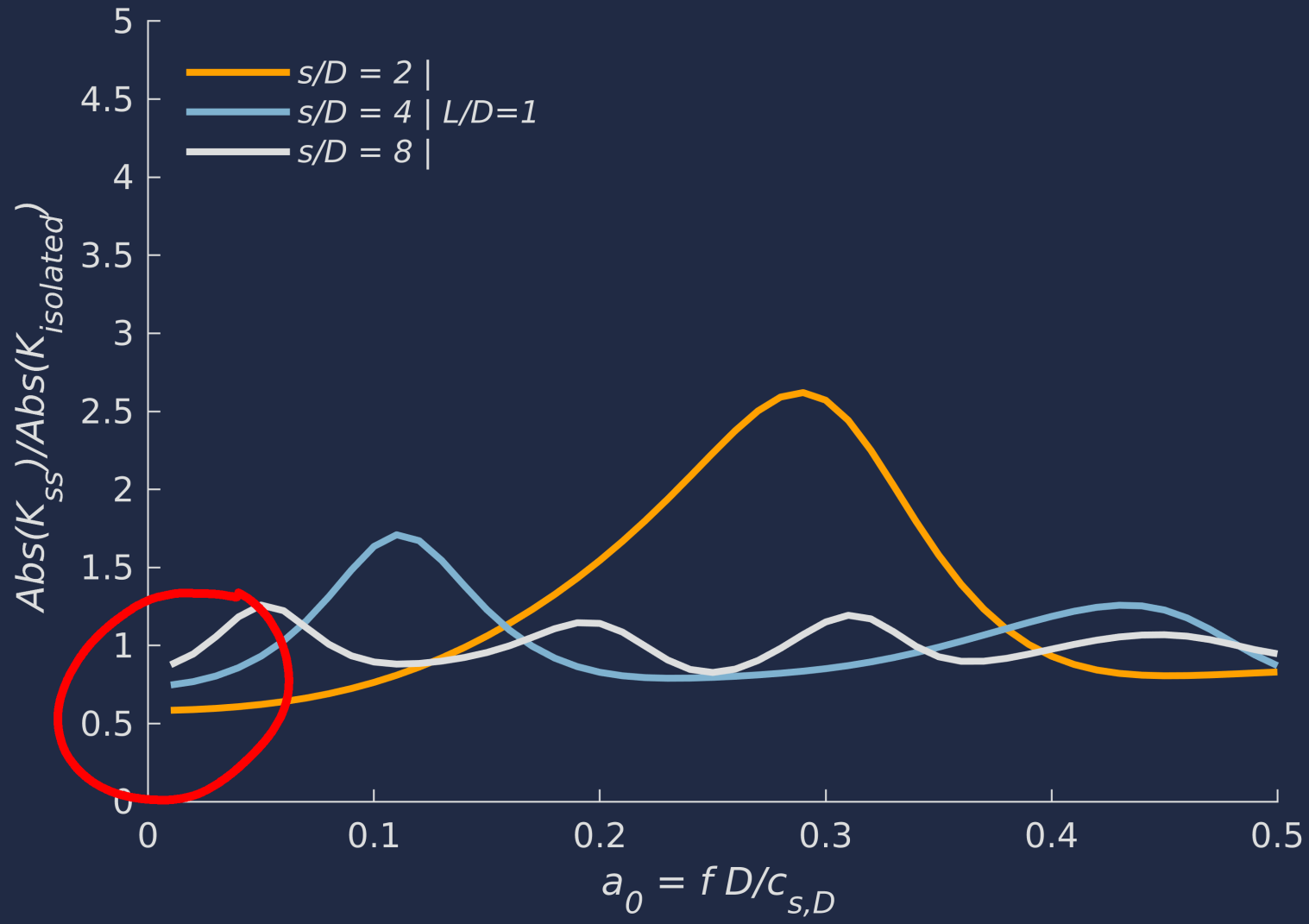

K_{SS} vs L/D vs s/D, $J = 100$, homogeneous soil

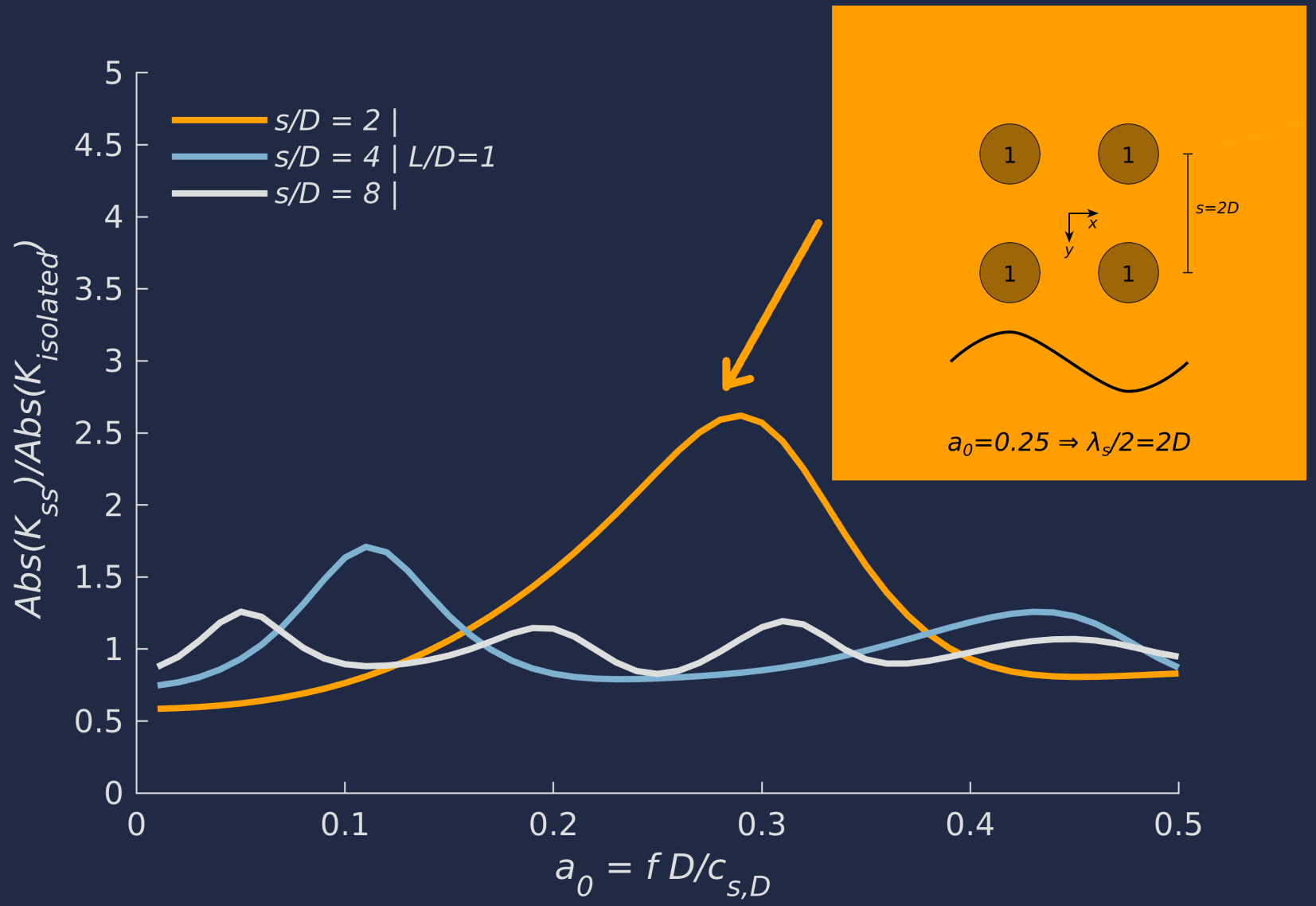

K_{SS} vs L/D vs s/D, $J = 100$, homogeneous soil

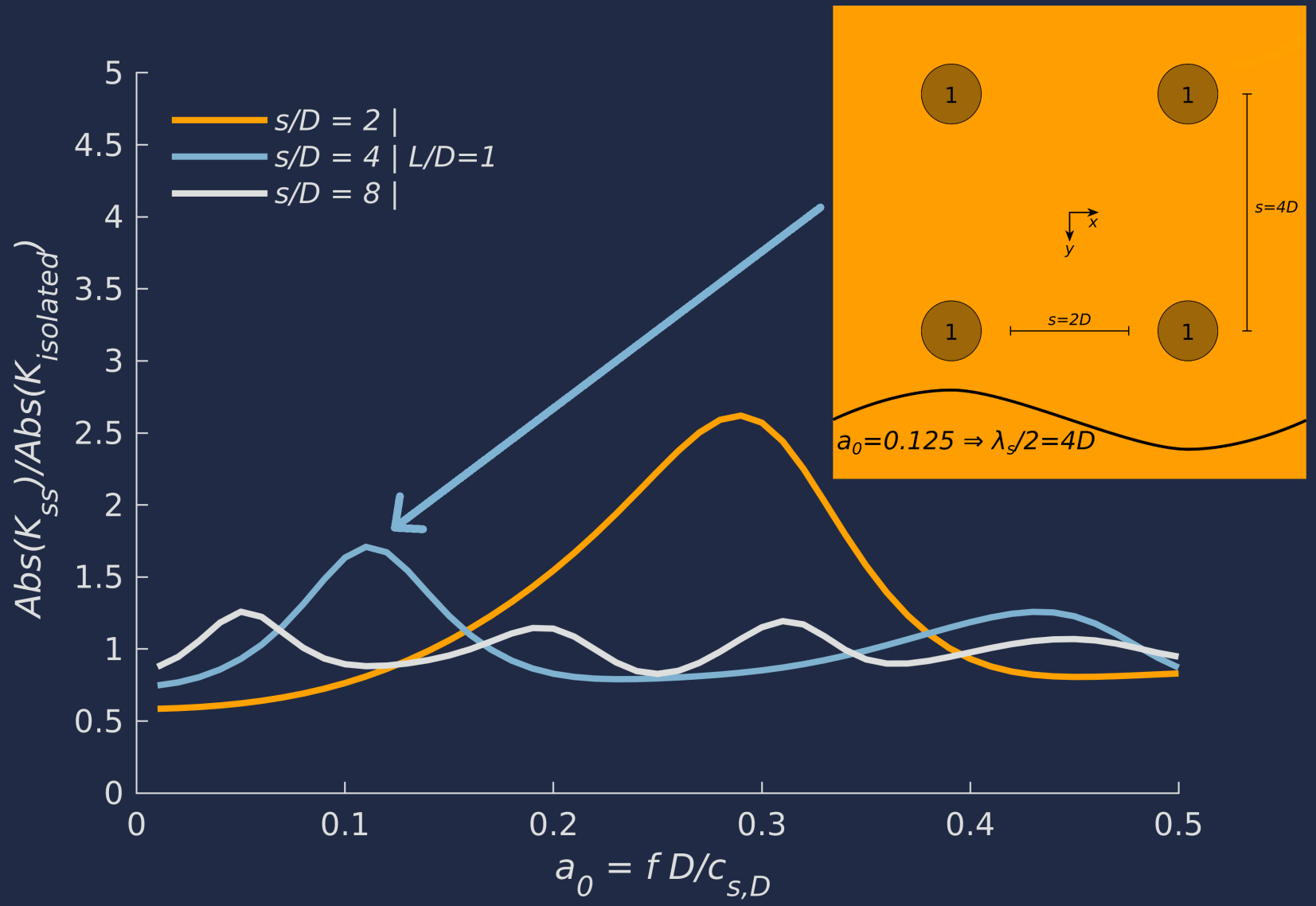

K_{SS} vs L/D vs s/D, $J = 100$, homogeneous soil

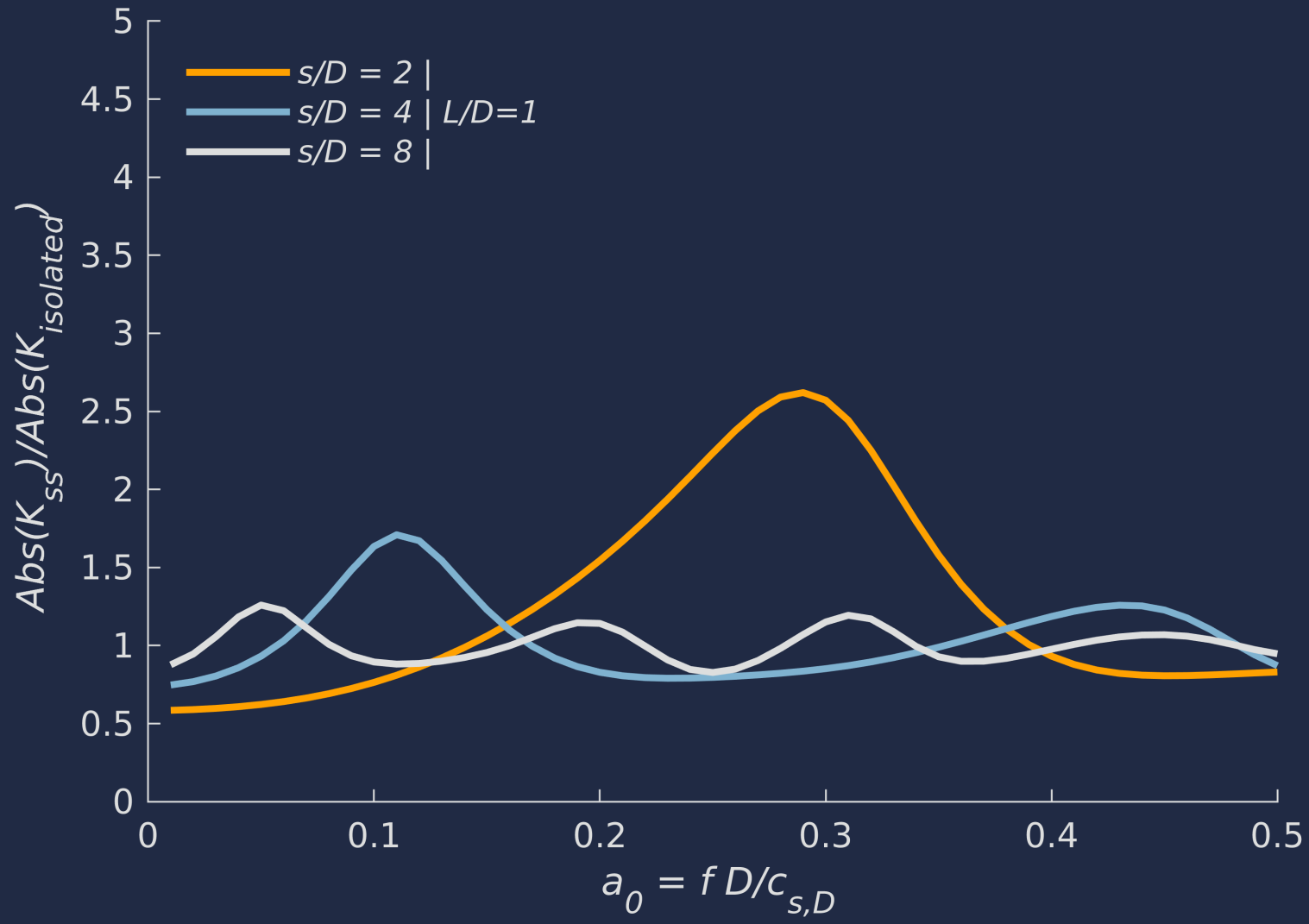

K_{SS} vs L/D vs s/D, $J = 100$, homogeneous soil

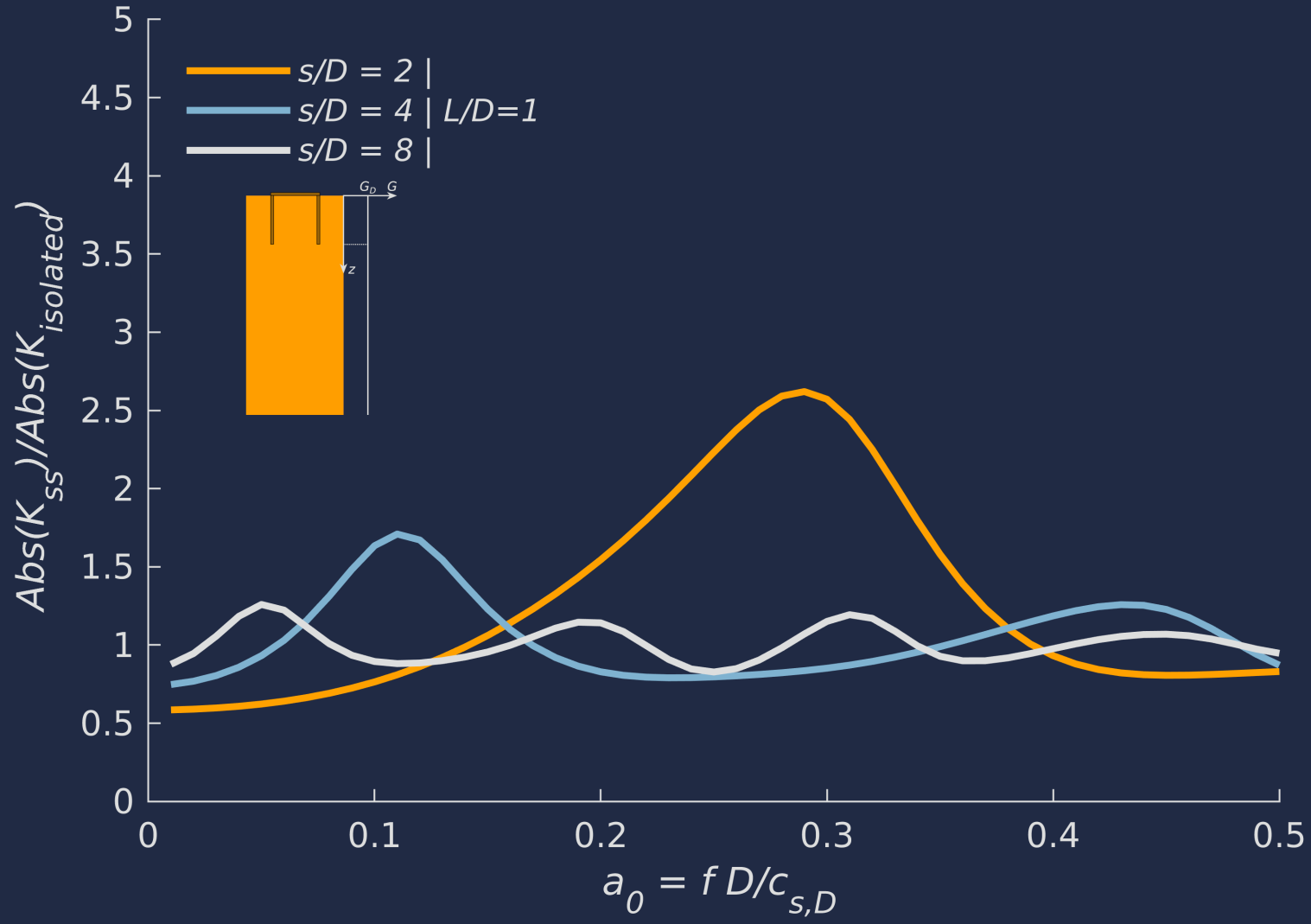

K_{SS} vs L/D vs s/D, $J = 100$, homogeneous soil

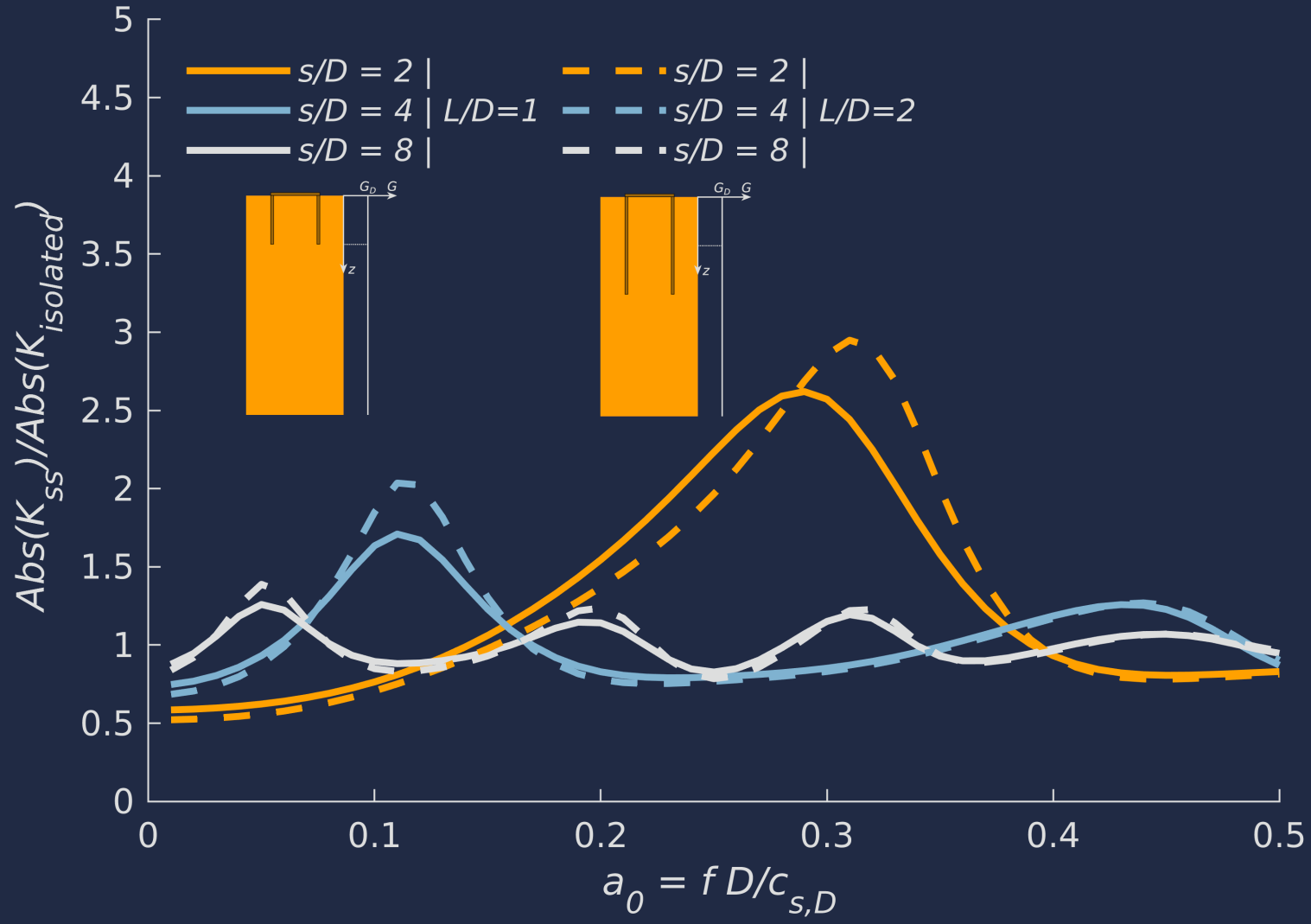

K_{SS} vs L/D vs s/D, $J = 100$, homogeneous soil

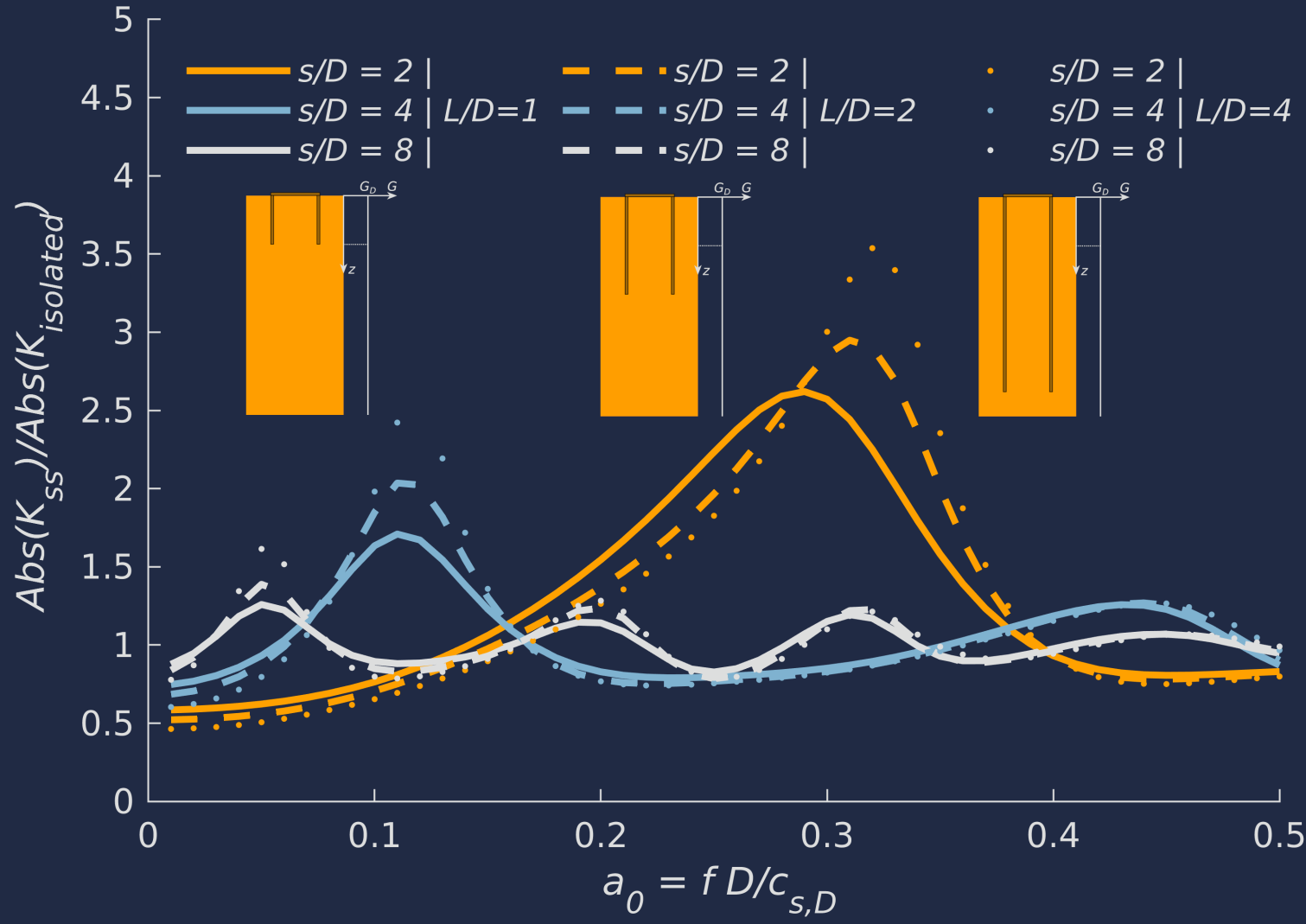

K_{SS} vs s/D vs m, $J = 100$, $L/D = 2$

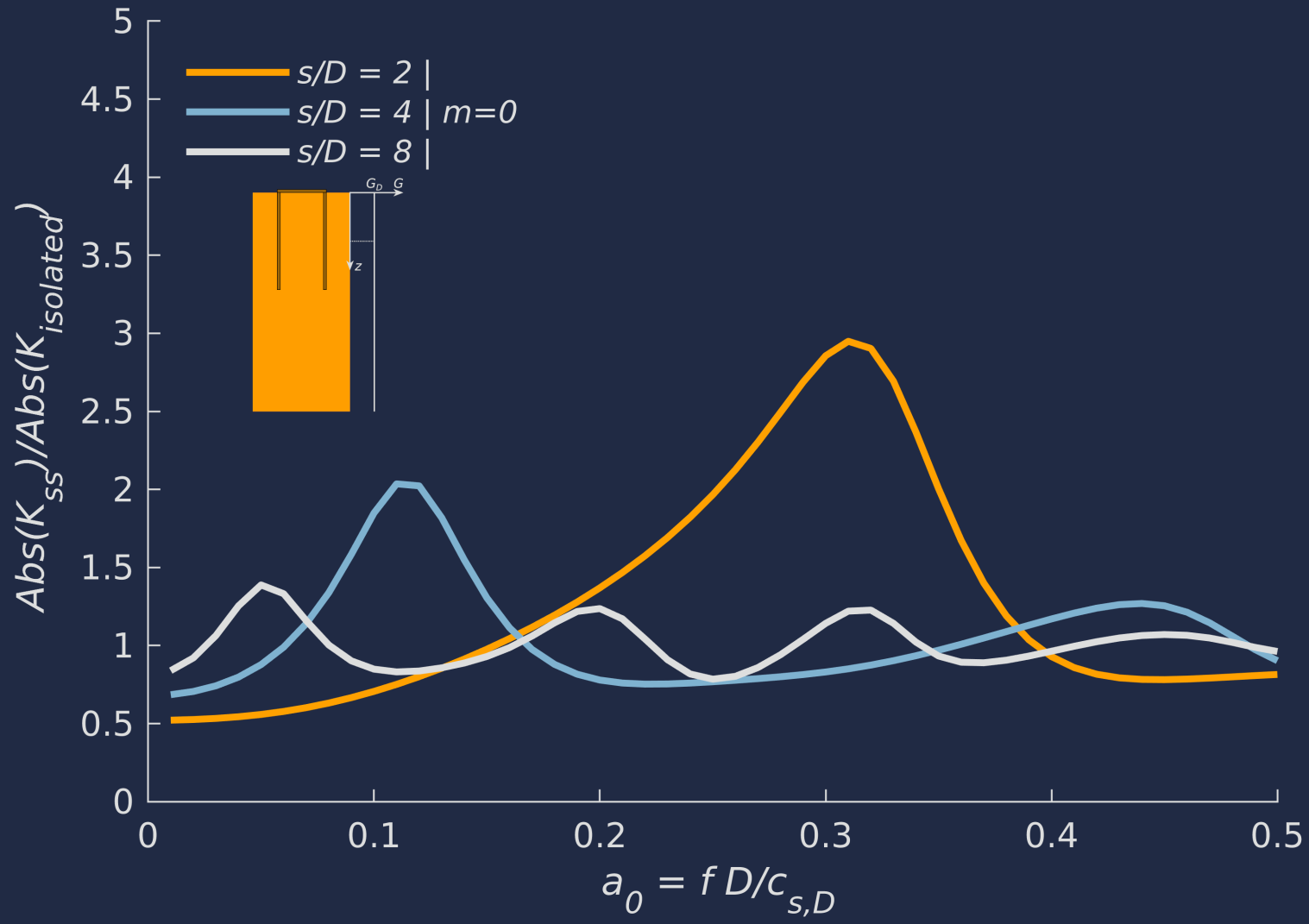

K_{SS} vs s/D vs m, $J = 100$, $L/D = 2$

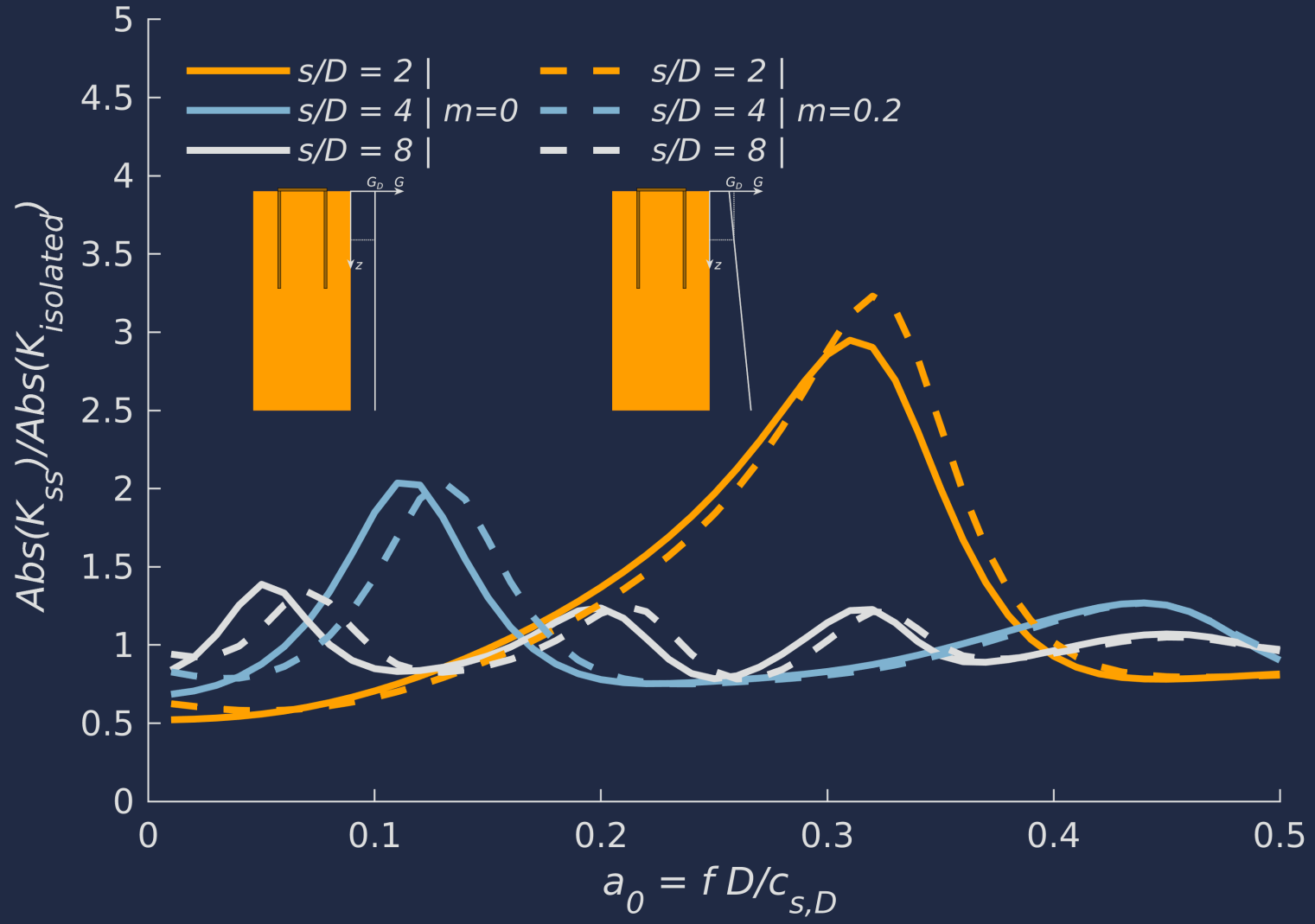

K_{SS} vs s/D vs m, $J = 100$, $L/D = 2$

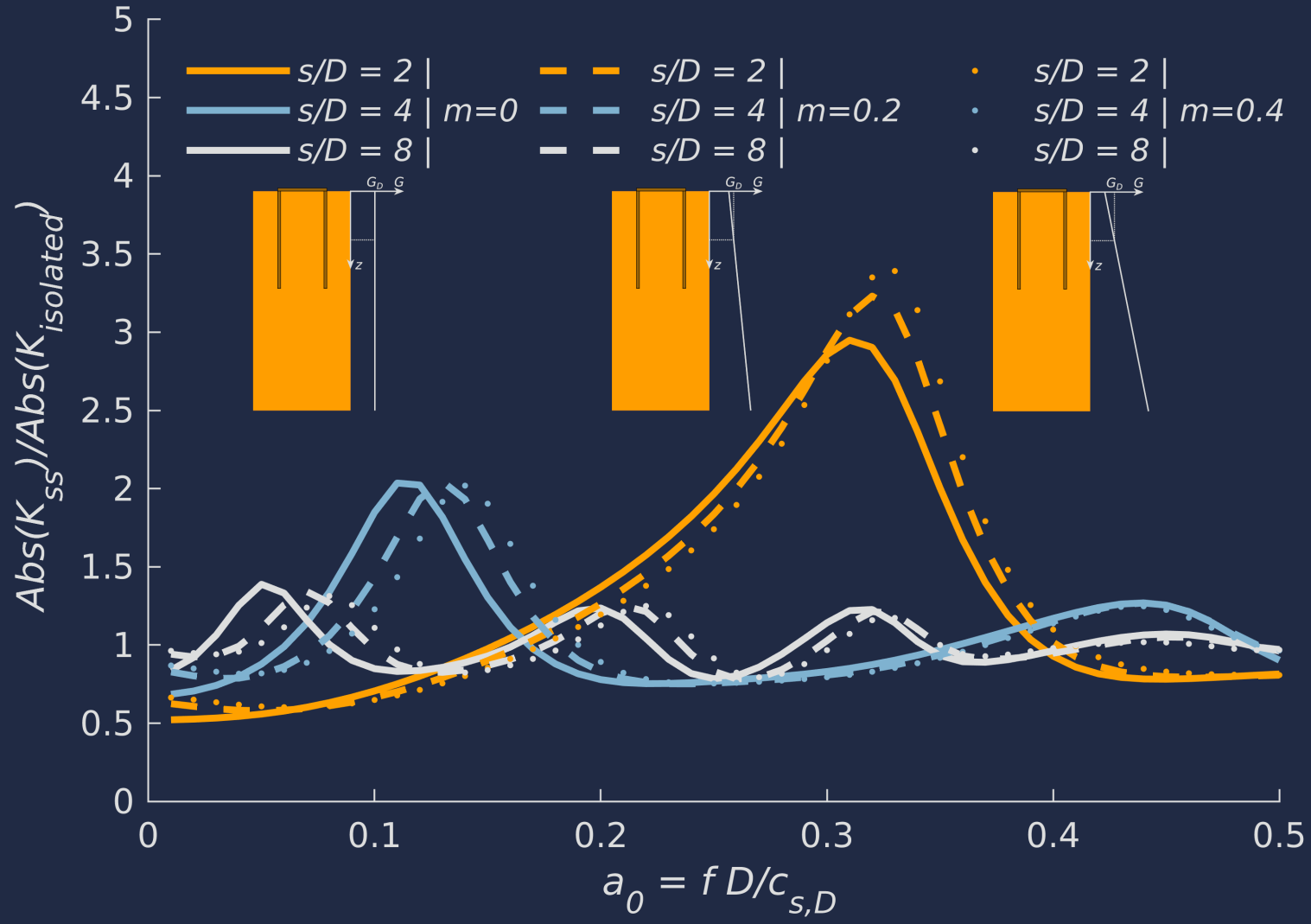

K_{aa} vs K_{sa} vs K_{ss}, $s/D = 8$, $L/D = 1$, homog.

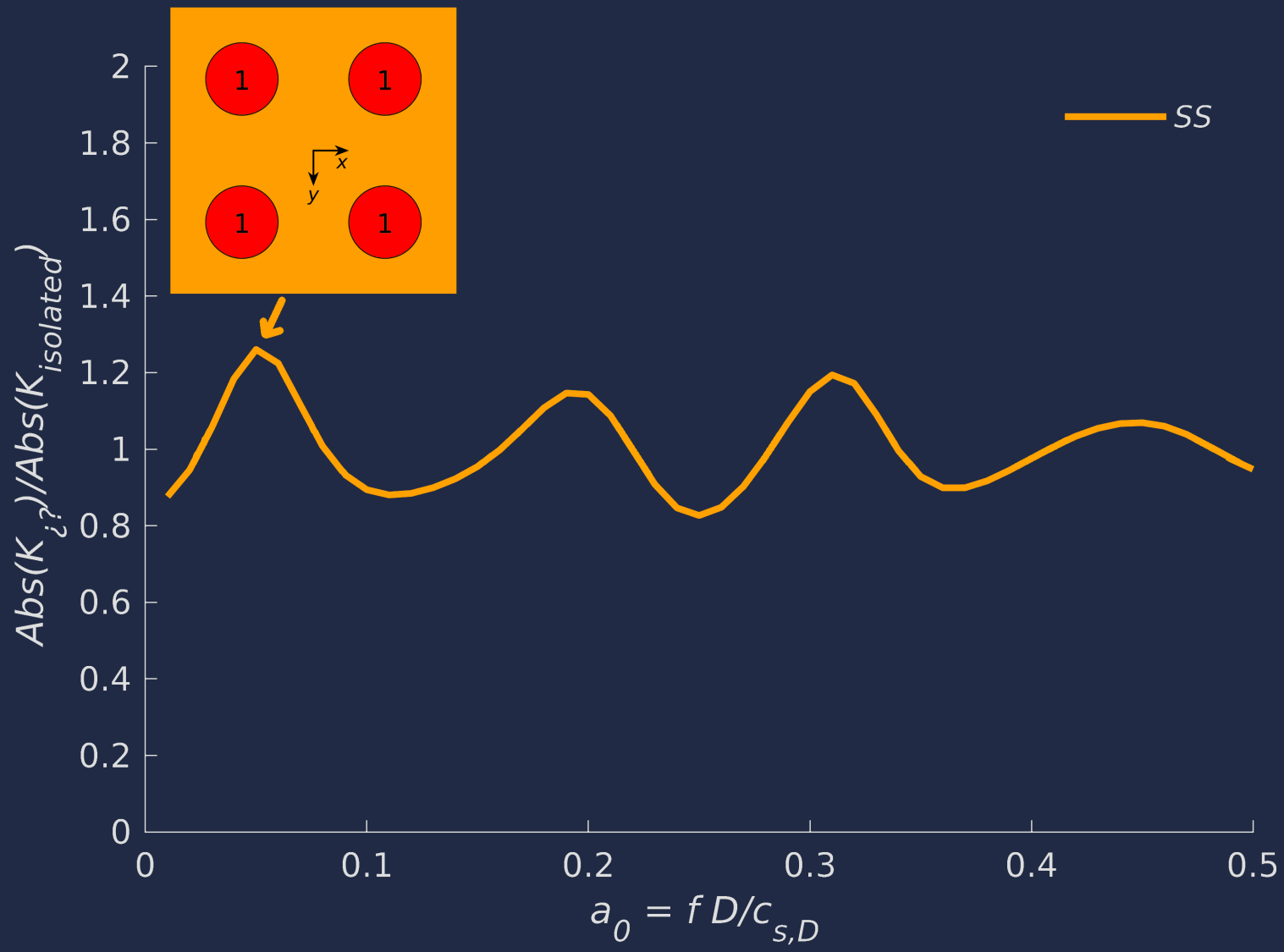

K_{aa} vs K_{sa} vs K_{ss}, $s/D = 8$, $L/D = 1$, homog.

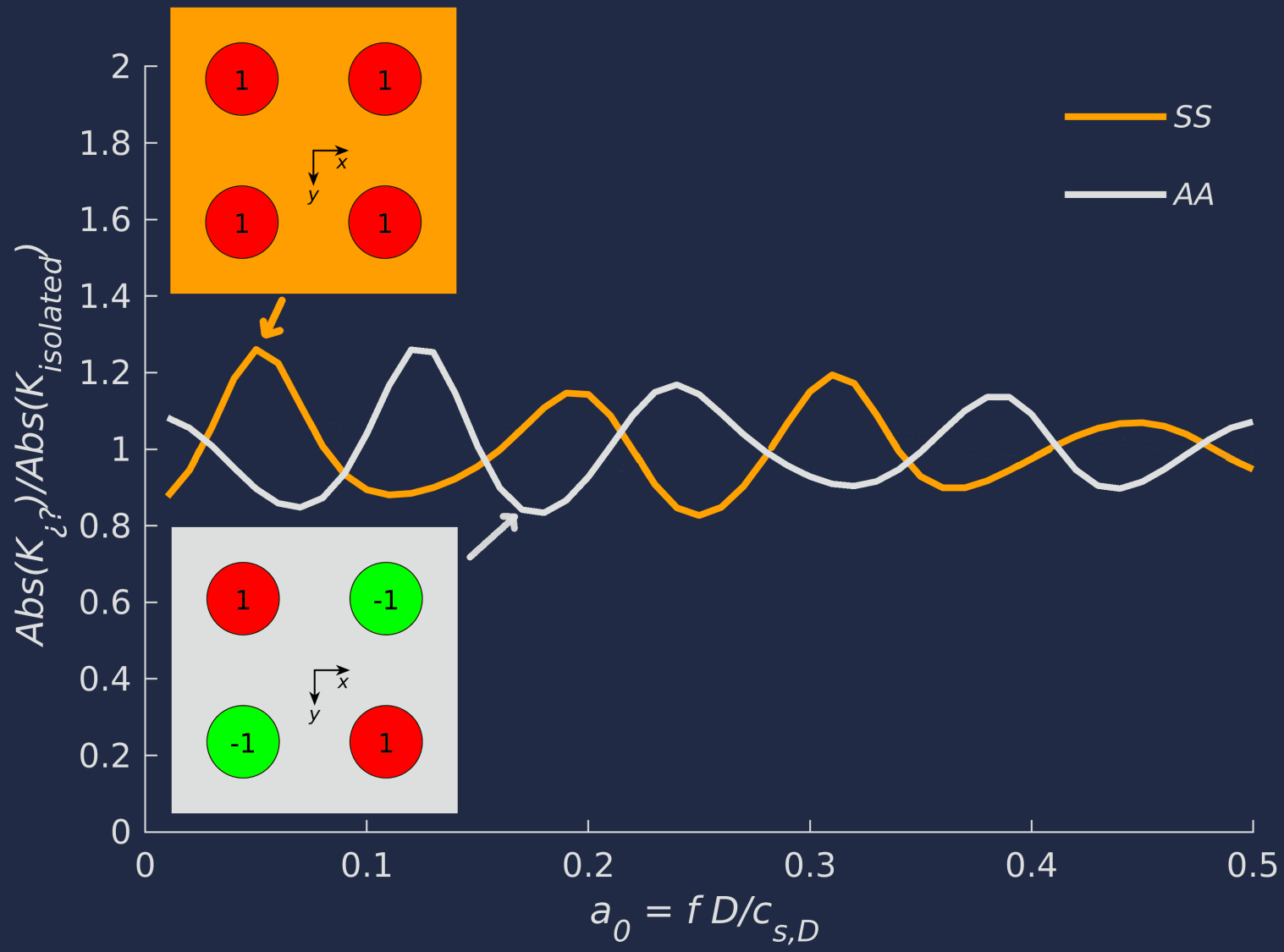

K_{aa} vs K_{sa} vs K_{ss}, $s/D = 8$, $L/D = 1$, homog.

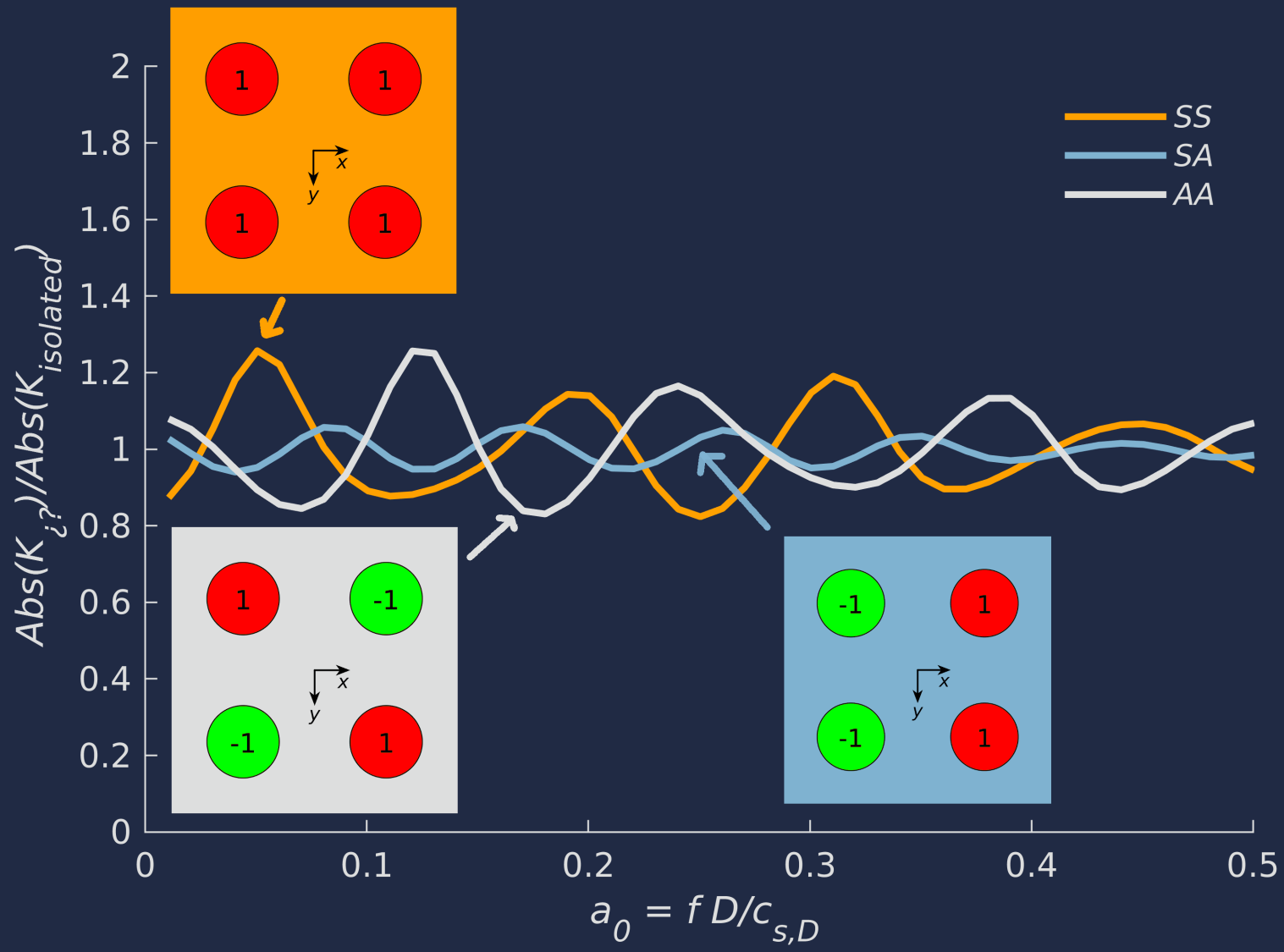

Vertical interaction (K_{11}, K_{12}, K_{13})

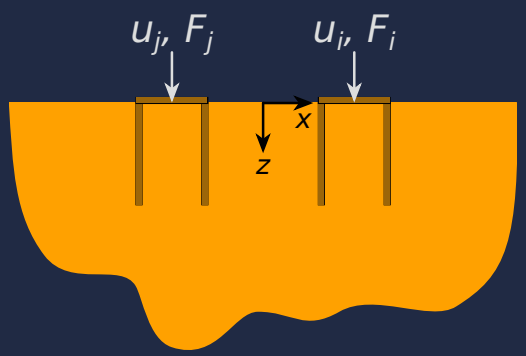

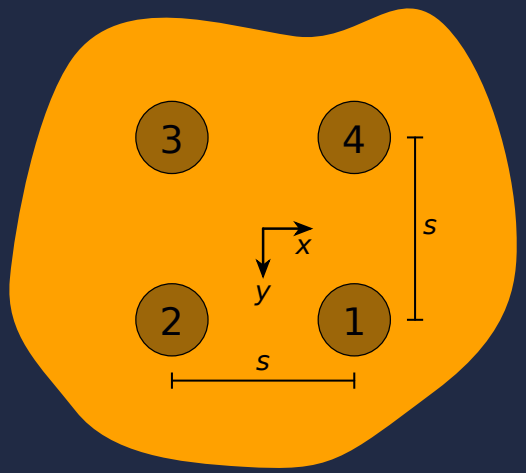

$$\begin{Bmatrix} F_1 \\ F_2 \\ F_3 \\ F_4 \end{Bmatrix} = \begin{bmatrix} K_{11} & K_{12} & K_{13} & K_{12} \\ & K_{11} & K_{12} & K_{13} \\ & & K_{11} & K_{12} \\ \text{sym.} & & & K_{11} \end{bmatrix} \begin{Bmatrix} u_1 \\ u_2 \\ u_3 \\ u_4 \end{Bmatrix}$$

Superposition of ss, sa, as ($\equiv$sa) and aa:

$$K_{11} = \frac{1}{4}\left(K_{ss} + 2K_{sa} + K_{aa}\right)$$

$$K_{12} = \frac{1}{4}\left(K_{ss} - K_{aa}\right)$$

$$K_{13} = \frac{1}{4}\left(K_{ss} - 2K_{sa} + K_{aa}\right)$$

K_{11}, K_{12}, K_{13} vs s/D, $L/D = 1$, $J = 100$, $m = 0$

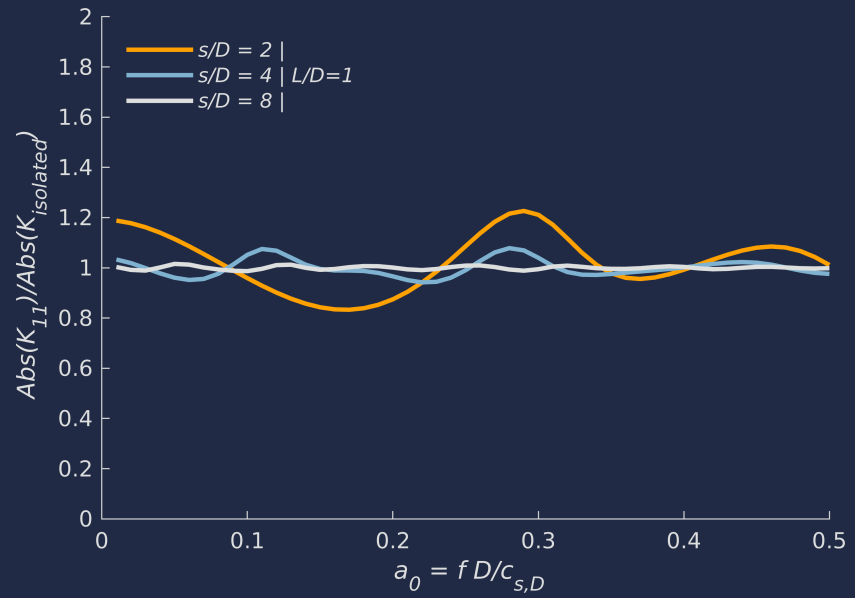

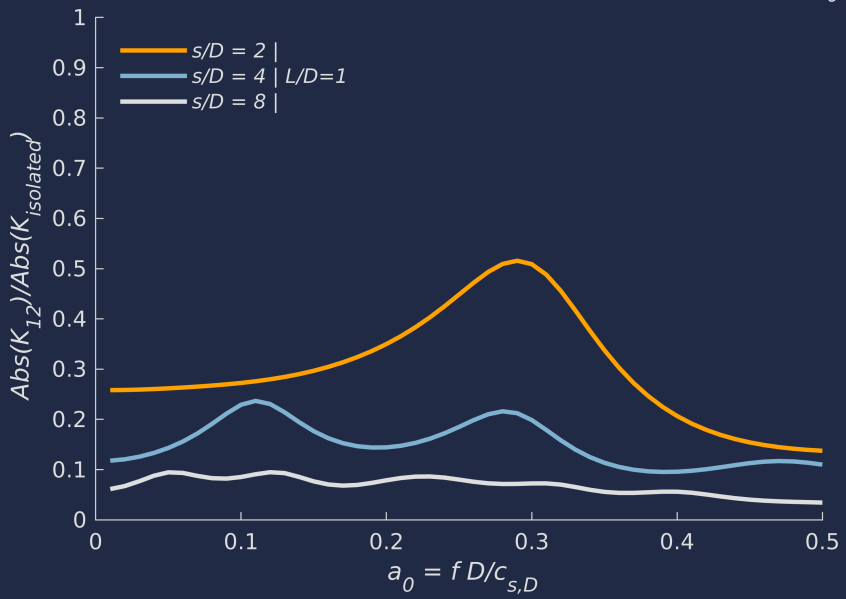

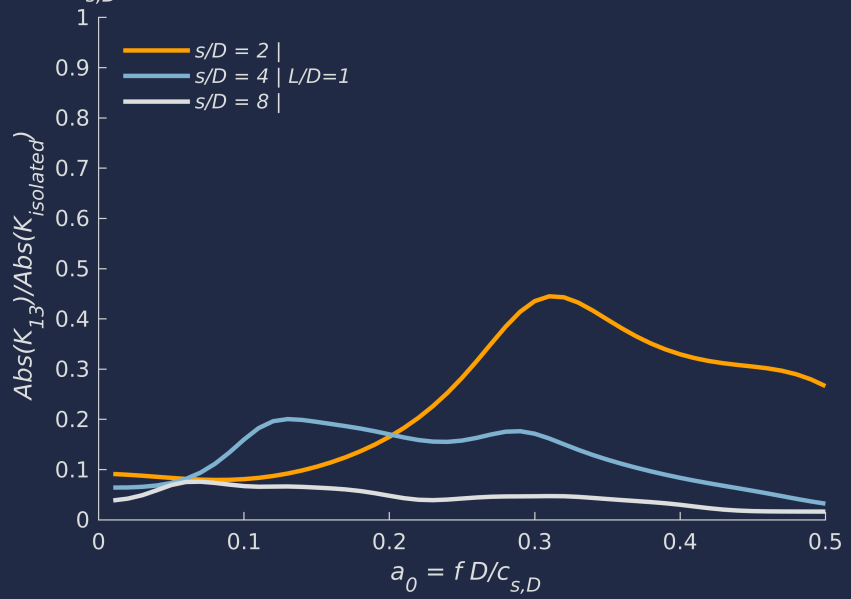

Outline

Conclusions

- Develop efficient BEM-FEM model for suction caissons in stratified soils

Conclusions

- Develop efficient BEM-FEM model for suction caissons in stratified soils
- Vertical dynamic interaction is dominated by shear waves

Conclusions

- Develop efficient BEM-FEM model for suction caissons in stratified soils
- Vertical dynamic interaction is dominated by shear waves
- Normalization by K_{isolated} is key:
  - L/D and J increases interaction strength
  - Similar behavior between homogeneous and Gibson
  - Criteria for neglecting interaction

Conclusions

- Develop efficient BEM-FEM model for suction caissons in stratified soils
- Vertical dynamic interaction is dominated by shear waves
- Normalization by K_{isolated} is key:
  - L/D and J increases interaction strength
  - Similar behavior between homogeneous and Gibson
  - Criteria for neglecting interaction
- Future: closed-form formulae or simplified methodology for engineering purposes

Acknowledgments

Research Project PID2020-120102RB-I00, funded by the Agencia Estatal de Investigación of Spain, MCIN/AEI/10.13039/501100011033:

ULPGC
Universidad de
Las Palmas de
Gran Canaria

Instituto Universitario de
Sistemas Inteligentes y Aplicaciones
Numéricas en Ingenierías

SIANI

División de Mecánica de los Medios Continuos y Estructuras:
`www.mmc.siani.es`